NAVAL POSTGRADUATE SCHOOL

Monterey, California

THESIS

A Surface Integral Algorithm for the Motion Planning of Nonholonomic Mechanical Systems

by

David P. Anderson

December 1992

Thesis Advisor: Ranjan Mukherjee

Approved for public release; distribution is unlimited

REPORT DOCUMENTATION PAGE

1a. REPORT SECURITY CLASSIFICATION Unclassified	1b. RESTRICTIVE MARKINGS
2a. SECURITY CLASSIFICATION AUTHORITY	3. DISTRIBUTION/AVAILABILITY OF REPORT Approved for public release; distribution is unlimited.
2b. DECLASSIFICATION/DOWNGRADING SCHEDULE	
4. PERFORMING ORGANIZATION REPORT NUMBER(S)	5. MONITORING ORGANIZATION REPORT NUMBER(S)
6a. NAME OF PERFORMING ORGANIZATION Naval Postgraduate School 6b. OFFICE SYMBOL (*If applicable*) 34	7a. NAME OF MONITORING ORGANIZATION Naval Postgraduate School
6c. ADDRESS (*City, State, and ZIP Code*) Monterey, CA 93943-5000	7b. ADDRESS (*City, State, and ZIP Code*) Monterey, CA 93943-5000
8a. NAME OF FUNDING/SPONSORING ORGANIZATION 8b. OFFICE SYMBOL (*If applicable*)	9. PROCUREMENT INSTRUMENT IDENTIFICATION NUMBER
8c. ADDRESS (*City, State, and ZIP Code*)	10. SOURCE OF FUNDING NUMBERS Program Element No. / Project No / Task No / Work Unit Accession Number

11. TITLE (*Include Security Classification*)
A Surface Integral Algorithm for the Motion Planning of Nonholonomic Mechanical Systems

12. PERSONAL AUTHOR(S) David P. Anderson

13a. TYPE OF REPORT	13b. TIME COVERED	14. DATE OF REPORT (*year, month, day*)	15. PAGE COUNT
Master's Thesis	From March 92 To December 92	December 92	67

16. SUPPLEMENTARY NOTATION
The views expressed in this thesis are those of the author and do not reflect the official policy or position of the Department of Defense or the U.S. Government.

17. COSATI CODES			18. SUBJECT TERMS (*continue on reverse if necessary and identify by block number*)
FIELD	GROUP	SUBGROUP	Holonomic, Nonholonomic, Scleronomic, Motion Constraints, Degrees of Freedom, Generalized Coordinates, Motion Planning

19. ABSTRACT (*continue on reverse if necessary and identify by block number*)

The number of coordinates needed to completely describe the configuration of a holonomic mechanical system is equal to the number of degrees of freedom possessed by that system. In contrast, nonholonomic systems always require more coordinates for their description than their are degrees of freedom due to the nonintegrable nature of the governing velocity constraints. The task of nonholonomic motion planning applied to a given system is to develop trajectories of the independent coordinate variables such that the entire system is driven to some desired point in its configuration space. An algorithm for constructing these trajectories is presented. In this algorithm, the independent variables are first converged to their desired values. The dependent variables are subsequently converged using closed trajectories of the independent variables. The requisite closed trajectories are planned using Stoke's Theorem which converts the problem of finding a closed path in the space of the independent variables to that of finding a surface area in that same space such that the dependent variables converge to their desired values as the independent variables traverse along the boundary of this surface area. The use of Stoke's Theorem simplifies the motion planning process and also answers important questions pertaining to the system. The salient features of the algorithm are apparent in the two examples discussed: a planar space robot and a disk rolling without slipping on a flat surface.

20. DISTRIBUTION/AVAILABILITY OF ABSTRACT	21. ABSTRACT SECURITY CLASSIFICATION	
☒ UNCLASSIFIED/UNLIMITED ☐ SAME AS REPORT ☐ DTIC USERS	Unclassified	
22a. NAME OF RESPONSIBLE INDIVIDUAL Ranjan Mukherjee	22b. TELEPHONE (*Include Area code*) (408) 646-2632	22c. OFFICE SYMBOL ME/Mk

DD FORM 1473, 84 MAR 83 APR edition may be used until exhausted
All other editions are obsolete

Approved for public release; distribution is unlimited.

A Surface Integral Algorithm for the Motion Planning of
Nonholonomic Mechanical Systems

by

David P. Anderson
Captain, United States Army
B.S., United States Military Academy, 1983

Submitted in partial fulfillment
of the requirements for the degree of

MASTER OF SCIENCE IN MECHANICAL ENGINEERING

from the

NAVAL POSTGRADUATE SCHOOL
December 1992

Author: 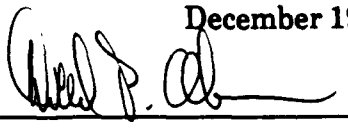
David P. Anderson

Approved by: 
Ranjan Mukherjee, Thesis Advisor


Matthew D. Kelleher, Chairman
Department of Mechanical Engineering

ABSTRACT

The number of coordinates needed to completely describe the configuration of a holonomic mechanical system is equal to the number of degrees of freedom possessed by that system. In contrast, nonholonomic systems always require more coordinates for their description than their are degrees of freedom due to the nonintegrable nature of the governing velocity constraints. The task of nonholonomic motion planning applied to a given system is to develop trajectories of the independent coordinate variables such that the entire system is driven to some desired point in its configuration space. An algorithm for constructing these trajectories is presented. In this algorithm, the independent variables are first converged to their desired values. The dependent variables are subsequently converged using closed trajectories of the independent variables. The requisite closed trajectories are planned using Stoke's Theorem which converts the problem of finding a closed path in the space of the independent variables to that of finding a surface area in that same space such that the dependent variables converge to their desired values as the independent variables traverse along the boundary of the surface area. The use of Stoke's Theorem simplifies the motion planning process and also answers important questions pertaining to the system. The salient features of the algorithm are apparent in the two examples discussed: a planar space robot and a disk rolling without slipping on a flat surface.

TABLE OF CONTENTS

I. INTRODUCTION

This thesis presents an algorithm for planning the motion of nonholonomic mechanical systems. The algorithm provides a means for calculating the coordinate trajectories required to drive a nonholonomic system from one point in its configuration space to some other desired point. The algorithm involves the use of Stoke's Theorem and therefore takes a surface integral approach to the problem. To enhance the reader's understanding of the algorithm, the discussion proceeds methodically. The goal of this first chapter is to clarify the nonholonomic motion planning problem and provide a conceptual overview of the surface integral approach to its solution. Chapter II. begins with a review of the mathematical details needed for a complete understanding of the algorithm, follows with a detailed discussion of the algorithm itself, and concludes with some notes on some of its more versatile features. In Chapter III., the surface integral algorithm is applied to two simple nonholonomic mechanical systems: a planar space robot and a disk rolling without slipping on a flat surface. These examples serve to validate the algorithm and, hopefully, solidify the reader's understanding of it. Finally, a summary is provided in Chapter IV. It is hoped that this methodical approach will provide the reader with an appreciation for the simplicity and utility of the surface integral algorithm for the motion planning of nonholonomic mechanical systems.

A. HOLONOMIC VERSUS NONHOLONOMIC SYSTEMS

The description of mechanical systems begins with a suitable choice of coordinates and an identification of the constraints of motion resulting from that choice. In the case of holonomic mechanical systems, coordinates can be chosen such that no

motion constraints arise. When the coordinates are chosen such that constraints of motion do arise, those constraints always entail a relationship between the coordinates themselves and not their derivatives. In contrast, nonholonomic mechanical systems always require constraints of motion to complete their description regardless of how the coordinates are chosen. This is because at least one of the constraints will involve a non-integrable relationship between the first derivatives of the coordinates. To further illustrate the difference between holonomic and nonholonomic mechanical systems, consider the two systems shown in Figs.1(a) and 1(b).

Figure 1(a) shows two particles m_1 and m_2 connected by a rigid, massless rod of length $(l_1 + l_2)$ on a two dimensional x-y plane. The center of mass of the system is shown. An infinite number of coordinate sets can be used to describe the configuration of this system. One choice might involve the use of the coordinates (x_c, y_c, θ) to specify the position of the center of mass of the system in the x-y plane and the orientation of the rod with respect to the vertical y axis. Such a choice completely describes the state of the mass-rod system and does not require any equations of constraint. A second choice of coordinate sets might involve the coordinates (x_1, y_1, x_2, y_2) to specify the positions of each mass in the x-y plane. Such a choice of coordinates requires the following constraint equation in order to completely describe the state of the system:

$$(x_2 - x_1)^2 + (y_2 - y_1)^2 = (l_1 + l_2)^2 \tag{1}$$

A third choice of coordinate sets might entail the coordinates $(x_1, y_1, x_2, y_2, x_c, y_c)$ to specify the positions of each mass as well as the center of mass in the x-y plane. Such a choice of coordinates requires three equations of constraint to completely describe the system:

$$(x_c - x_1)^2 + (y_c - y_1)^2 = l_1^2 \tag{2a}$$

$$(x_2 - x_c)^2 + (y_2 - y_c)^2 = l_2^2 \tag{2b}$$

$$(x_2 - x_1)^2 + (y_2 - y_1)^2 = (l_1 + l_2)^2 \tag{2c}$$

Obviously, the possible number of coordinate sets that might be chosen to describe this system are endless. However, all possible coordinate sets share one common feature: they result in either no constraints of motion or constraints of motion which relate the coordinates of the system and not their derivatives. Hence, the rod-mass system of Fig.1(a) is a holonomic mechanical system.

Consider now the system shown in Fig.1(b). This system consists of a disk of radius r rolling without slipping on the x-y plane. A set of coordinates which might be chosen to describe the location of a point P on the disk is (x, y, θ, α) where x and y describe the location of the disk's point of contact with the ground, θ describes the angle a radial line through point P makes with the vertical z axis, and α describes the angle the disk's instantaneous direction of motion on the x-y plane makes with the horizontal y axis. Such a choice of coordinates results in the following two equations of constraint:

$$\dot{x} = r\dot{\theta}\sin\alpha \tag{3a}$$

$$\dot{y} = r\dot{\theta}\cos\alpha \tag{3b}$$

Note that Eqs.(3a) and (3b) above relate the derivatives of the coordinates to each other and not the coordinates themselves. Furthermore, since α is an independent function of time, Eqs.(3a) and (3b) cannot be integrated to yield relationships between the coordinates (the conditions for nonintegrability of a differential expression will be discussed in Chapter II.A.1). For this reason, Eqs.(3a) and (3b) are termed nonholonomic constraints on the disk of Fig.1(b), and the disk itself is said to be a nonholonomic mechanical system. All nonholonomic mechanical systems share this feature: the constraints of motion relate the velocities of the system and cannot be integrated to yield relationships between the coordinate positions.

This feature of nonholonomic systems is unique and gives rise to the nonholonomic motion planning problem.

B. THE NONHOLONOMIC MOTION PLANNING PROBLEM

In the previous section, it was shown that nonholonomic mechanical systems are governed by constraints of motion which involve nonintegrable relationships between the velocities of the system. In this section, it will be shown how this feature of nonholonomic systems gives rise to the nonholonomic motion planning problem. To understand this problem, a number of terms must first be discussed.

The configuration space of a mechanical system is the space defined by the minimum number of coordinates needed to completely describe that system. The dimension of the configuration space is the number of those coordinates. The degrees of freedom of a mechanical system is defined as the difference between the number of coordinates used to describe the system and the number of independent equations of constraint arising from that description. In more specific terms, given a mechanical system described by n coordinates and m independent equations of constraint, the number of degrees of freedom possessed by the system is equal to $n - m$. The number of degrees of freedom possessed by a given system is a fixed number and is completely independent of the coordinate system chosen. Finally, the number of independent coordinates available to a given mechanical system is synonomous with the number of degrees of freedom of the system. Additional coordinates over and above this number are always dependent.

Consider now the holonomic rod-mass system of Fig.1(a). Note that it is a three degree of freedom system since, regardless of how the coordinates are chosen, the number of coordinates minus the number of independent constraints is always equal to three. Likewise, the number of independent coordinates available to the system is also equal to three although for any given set of coordinates, the choice of which

are independent and which are dependent is both physically and mathematically arbitrary. Now consider the nature of the holonomic constraints described by Eqs.(1), (2a), (2b), and (2c). Note that because these equations all entail a direct relationship between the coordinates themselves, specification of the values of any three of the variables uniquely determines the values of any remaining variables. In other words, regardless of which coordinate system is chosen, specification of the values of the independent coordinates uniquely determines the value of the dependent coordinates. As a result, only the values of the independent coordinates are needed in order to completely specify the configuration of the system. This is true of all holonomic mechanical systems and because the number of independent coordinates available to a given system is equal to the number of degrees of freedom possessed by that system, the dimension of the configuration space of a holonomic system is always equal to its number of degrees of freedom.

Now consider the nonholonomic rolling disk of Fig.1(b) and its accompanying constraint equations, Eqs.(3a) and (3b). Note that it is a two degree of freedom system since the number of coordinates used to describe the system minus the number of independent equations of constraint is equal to two. The coordinates x and y are clearly the dependent variables since their values can only be changed by either rolling or both rolling and turning the disk. Note however that the values of x and y are not uniquely determined by the constraint equations given the values of the independent variables θ and α. This is due to the fact that the constraint equations represent non-integrable relationships between the velocities of the system and not the coordinates themselves. As a result, the values of all four coordinates must be specified separately in order to completely describe the configuration of the rolling disk. Unlike the holonomic constraint equations of the rod-mass system, the nonholonomic constraint equations of the rolling disk do not restrict the dimension of the configuration space

of the system. This is a unique feature of nonholonomic mechanical systems and forms the heart of the nonholonomic motion planning problem: their ability to access a configuration space of higher dimension than their number of degrees of freedom. The nonholonomic motion planning problem can therefore be stated as follows: given a system described by n coordinates and m nonholonomic constraints, how does one drive all n of the coordinates from some initial set of values to some desired set of values in spite of the system having only $n - m$ degrees of freedom? The answer to this question has been sought by numerous researchers and a variety of solutions have been proposed. In the next section, a brief survey of some of these solution techniques will be presented.

C. LITERATURE SURVEY

The nonholonomic motion planning problem has been the focus of attention of various researchers in the recent past. Specifically, researchers have considered the questions of how a falling cat manages to always land on its feet [Ref. 1, Ref. 2: pp. 25-30] and how an astronaut might use those same principles to reorient himself during a spacewalk [Ref. 3]. Researchers have also considered the problems of mobile wheeled robot navigation [Ref. 4, Ref. 5], parking a front wheel drive car [Ref. 2: pp. 89-91, Ref. 6: pp. 8-11, Ref. 7: pp. 17-19], parking a cart with multiple trailers [Ref. 6: pp. 11-13, Ref. 7: pp. 29-30, Ref. 8], controlling a unicycle or rolling disk [Ref. 2: pp. 83-89, Ref. 6: pp. 6-8], controlling a satellite with rotors instead of gas jets [Ref. 2: pp. 21-25], dextrous manipulation with robotic fingers [Ref. 9], and reconfiguration of a space structure or space manipulator using only internal motion [Ref. 10, Ref. 11]. Each of these researchers have explored various aspects of the nonholonomic motion planning problem and have developed unique solutions to it.

Kane, Headrick, and Yatteau [Ref. 3] conducted experiments to determine the feasibility of a spacewalking astronaut to reorient himself through arm motion only.

The nonholonomy of an astronaut or any freefloating spacecraft derives from the principle of angular momentum conservation. While these researchers did not approach this problem in the broad context of nonholonomic motion planning, their research pointed the way towards a number of possible solution techniques.

The problem of controlling a multi degree of freedom space manipulator was first addressed by Vafa and Dubowsky [Ref. 11]. The dynamic coupling between the joints of a space manipulator and the vehicle to which it is attached often results in an undesirable drift of the vehicle when the joints are actuated. Vafa and Dubowsky proposed using small cyclic motions of the manipulator joints to control this drift. The problem was also tackled by Nakamura and Mukherjee [Ref. 10] who showed that the vehicle orientation as well as the joint angles could be brought to their desired configurations by executing appropriate trajectories of the joint angles. The trajectories were planned using a Lyupanov function and by adopting a bidirectional approach.

The nonholonomic nature of a car or cart with multiple trailers evolves along the same lines as that of the rolling disk discussed in the previous sections. Laumond [Ref. 8] studied the multibody car system and concluded its controllability by showing that the rank of the control Lie Algebra is equal to the dimension of the state space at every point in the state space. Murray and Sastry [Ref. 7: pp. 29-30] also studied the problem. They showed that the dependent variables of the system could be brought to their desired values by executing closed trajectories of the independent variables. The closed trajectories were planned using a scheme involving sinusoids.

While the research discussed above sheds light on various aspects of the nonholonomic motion planning problem, none of the methods, algorithms, or concepts developed thus far completely solve the problem. A general scheme, applicable to a

wide range of nonholonomic mechanical systems, has not yet been presented. Additionally, a global scheme for addressing important questions such as motion planning in the presence of additional constraints, the reachability of a given system, and repeatability is conspicuously absent from the literature. The surface integral algorithm represents a new approach. Not only is it applicable to a large class of nonholonomic systems, but its implementation also leads to definitive answers to the questions posed above. In the next section, a conceptual overview of the algorithm will be presented.

D. OVERVIEW OF THE SURFACE INTEGRAL ALGORITHM

To gain a basic understanding of the surface integral approach to the motion planning of nonholonomic systems, consider again the rolling disk, this time shown in Fig.2(a). Suppose it is desired that the disk change its coordinates from (x, y, θ, α) to $(x_d, y_d, \theta, \alpha)$. A very simple way of accomplishing this would be to first roll the disk forward along path segment AO, and then roll the disk backwards along path segment OB. As shown in the figure, the end result of such a maneuver would be that the coordinates θ and α remain constant while the coordinates x and y move to their desired values x_d and y_d. Such an operation involves the execution of a *closed loop trajectory* in the θ-α plane , shown in Fig.2(b), to achieve the desired change in x and y. In more general terms then, it appears as though it is possible for nonholonomic mechanical systems to achieve a desired configuration of the dependent variables simply by executing an appropriate closed loop path in the space of the independent variables. It therefore follows then, that to converge all of the configuration variables of a nonholonomic system from one set of values to another, one might first converge the independent variables from their initial values to their desired values without being concerned about the evolution of the dependent variables. One could then execute an appropriate closed loop path in the space of the independent variables to converge the dependent variables to their desired values.

The technique described above leaves one critical question unanswered. How does one calculate an appropriate closed loop path? The surface integral algorithm is the answer. In this method, the problem of finding a closed loop path in the space of the independent variables is transformed into the problem of determining a surface area in that same space such that the dependent variables converge to their desired values as the independent variables traverse around the boundary of the surface area. The required transformation is accomplished by applying Stoke's Theorem to the differential form of the nonholonomic constraint equations.

To summarize, the essential features of the surface integral algorithm for the motion planning of nonholonomic systems can be stated as follows: all of the configuration variables of a nonholonomic mechanical system are brought to their desired values by first converging the independent variables and then by executing a closed loop path in the space of the independent variables to converge the dependent variables. The requisite closed loop path is calculated by applying Stoke's Theorem to the differential form of the nonholonomic constraint equations.

In the next chapter, Stoke's Theorem and other mathematical details needed for a full understanding of the surface integral algorithm will be reviewed. Following that, a detailed mathematical description of the surface integral algorithm will be presented. Finally, the algorithm's ability to answer important questions pertaining to the system will be discussed.

II. THE SURFACE INTEGRAL APPROACH TO THE NONHOLONOMIC MOTION PLANNING PROBLEM

A. MATHEMATICAL PRELIMINARIES

1. Nonintegrability of Nonholonomic Constraints

In Chapter I., nonholonomic constraints were described as constraints which involved a nonintegrable relationship between the first derivatives of the coordinates. An obvious question is how does one determine whether or not a given constraint is nonintegrable? To answer, the constraint equation must first be recast into differential form. Taking the constraint described by Eq.(1) for example, and differentiating with respect to time yields

$$(x_2 - x_1)(\dot{x}_2 - \dot{x}_1) + (y_2 - y_1)(\dot{y}_2 - \dot{y}_1) = 0$$

Rewriting in differential form and designating x_2 as the dependent variable yields

$$(x_2 - x_1)(dx_2 - dx_1) + (y_2 - y_1)(dy_2 - dy_1) = 0$$

$$dx_2 = (\frac{y_1 - y_2}{x_2 - x_1})dy_2 - (\frac{y_1 - y_2}{x_2 - x_1})dy_1 + dx_1 \tag{4}$$

Equation (4) represents the constraint described by Eq.(1) recast into differential form.

Recasting the nonholonomic constraints of the rolling disk into differential form is a simpler task.

$$\dot{x} = r\dot{\theta}\sin\alpha \quad \longrightarrow \quad dx = (r\sin\alpha)d\theta \tag{5a}$$

$$\dot{y} = r\dot{\theta}\cos\alpha \quad \longrightarrow \quad dy = (r\sin\alpha)d\theta \tag{5b}$$

The above discussion helps to illustrate the fact that any set of constraint equations, be they holonomic or nonholonomic, can be written in the following general form

$$\sum_{i=1}^{n} a_{ji}\, dq_i + a_{jt}\, dt = 0, \qquad j = 1, 2, \cdots m \tag{6}$$

where the q's represent the generalized coordinates, t represents time, and the a's are, in general, functions of the q's and t. In Eqs.(4), (5a), and (5b) the time coordinate does not appear explicitly. This is a property of what are termed scleronomic systems, and only mechanical systems of this type will be considered in this discussion. As before, n represents the number of generalized coordinates used to describe the system and m represents the number of independent constraint equations.

With the constraint equations in differential form, a simple test can be applied to determine whether or not the equations are integrable. Strictly speaking, a differential expression is integrable if and only if it is an exact differential or can be converted into an exact differential by multiplying through with an integrating factor. In, more specific terms, it can be shown that the necessary and sufficient condition for the integrability of the differential expression

$$v_1 dx + v_2 dy + v_3 dz = 0 \tag{7a}$$

where v_1, v_2, and v_3 are continuous functions of x, y, and z in a domain D of space is that

$$v_1 \left(\frac{\partial v_2}{\partial z} - \frac{\partial v_3}{\partial y} \right) + v_2 \left(\frac{\partial v_3}{\partial x} - \frac{\partial v_1}{\partial z} \right) + v_3 \left(\frac{\partial v_1}{\partial y} - \frac{\partial v_2}{\partial x} \right) = 0 \tag{7b}$$

In the more general case, the necessary and sufficient condition that the differential constraint in n variables

$$v_1\, dx_1 + v_2\, dx_2 + \cdots + v_n\, dx_n = 0 \tag{8a}$$

is integrable is that the set of equations

$$v_\nu \left(\frac{\partial v_\mu}{\partial x_\lambda} - \frac{\partial v_\lambda}{\partial x_\mu}\right) + v_\mu \left(\frac{\partial v_\lambda}{\partial x_\nu} - \frac{\partial v_\nu}{\partial x_\lambda}\right) + v_\lambda \left(\frac{\partial v_\nu}{\partial x_\mu} - \frac{\partial v_\mu}{\partial x_\nu}\right) = 0$$

$$(\lambda, \mu, \nu = 1, 2, \cdots, n) \qquad (8b)$$

are satisfied simultaneously and identically. [Ref. 12]

Applying this criterion to Eq.(4) shows that this constraint is in fact integrable and therefore holonomic. Applying this criterion to Eqs.(5a) and (5b) shows that they are not integrable and therefore nonholonomic.

2. Relevant Theorems

In this part of the chapter, two important mathematical theorems will be reviewed. The first is Stoke's Theorem used for the transformation of line integrals into surface integrals and vice versa. The second concerns the path independence of line integrals. Stoke's Theorem will serve as the principal mathematical tool for determining the required closed loop path needed to converge the dependent variables. The theorem regarding the path independence of line integrals will be crucial to the demonstration that the dependent variables can in fact be driven to any desired configuration from any other.

a. *Stoke's Theorem*

Let S be a piecewise smooth oriented surface* in space and let the boundary of S be a piecewise smooth closed curve C. Let $\boldsymbol{v}(x, y, z)$ be a continuous vector function which has continuous first partial derivatives in a domain in space which contains S.

* If a surface S has a unique normal whose direction depends continuously on the points of S, then S is called a smooth oriented surface. If S is not smooth but can be subdivided into finitely many smooth portions, then it is called a piecewise smooth oriented surface.

Then

$$\oint_C v_t \, ds = \int\int_S \boldsymbol{n}^T (\nabla \times \boldsymbol{v}) \, dA \tag{9}$$

where $\boldsymbol{n}$ is the unit vector normal to the surface S on that side of S which is taken as the positive side. The positive direction along C is then defined as the direction along which an observer, travelling on the positive side of S, would proceed in keeping the enclosed area to his left. Refer to Fig.3(a). v_t is the component of $\boldsymbol{v}$ in the direction of the tangent vector of C. [Ref. 13: p. 364]

If the direction cosines of the unit vector $\boldsymbol{n}$ normal to the surface S are $\cos\alpha$, $\cos\beta$, and $\cos\gamma$, and if $\boldsymbol{v} = v_1\boldsymbol{i} + v_2\boldsymbol{j} + v_3\boldsymbol{k}$, then Stoke's Theorem can be written as

$$\oint_C (v_1 \, dx + v_2 \, dy + v_3 \, dz) =$$

$$\int\int_S \left[\left(\frac{\partial v_3}{\partial y} - \frac{\partial v_2}{\partial z} \right) \cos\alpha + \left(\frac{\partial v_1}{\partial z} - \frac{\partial v_3}{\partial x} \right) \cos\beta + \left(\frac{\partial v_2}{\partial x} - \frac{\partial v_1}{\partial y} \right) \cos\gamma \right] dA \tag{10}$$

If the space under consideration is restricted to the x-y plane, then Eq.(10) simplifies to the form

$$\oint_C (v_1 \, dx + v_2 \, dy) = \int\int_S \left(\frac{\partial v_2}{\partial x} - \frac{\partial v_1}{\partial y} \right) dx \, dy \tag{11}$$

which is essentially a statement of Green's Theorem [Ref. 13: p. 336].

For Eq.(11), the positive direction along the closed curve C is shown in Fig.3(b). This directly follows from Eq.(10) where the values of α, β, and γ were taken to be $\pi/2$, $\pi/2$, and 0 respectively. The direction of the closed curve C in Eq.(11) may be changed by using $(\alpha, \beta, \gamma) = (\pi/2, \pi/2, \pi)$ in Eq.(10). This will lead to a change in sign of the surface integral in Eq.(11).

b. The Path Independence of Line Integrals

Let $\boldsymbol{v} = v_1\boldsymbol{i} + v_2\boldsymbol{j} + v_3\boldsymbol{k}$, and let v_1, v_2, and v_3 be continuous functions of x, y, and z in a domain D of space. Then the line integral

$$\int_C (v_1 \, dx + v_2 \, dy + v_3 \, dz) \tag{12}$$

is independent of path if and only if the differential form under the integral sign is exact in D, or equivalently the integral is zero for every simple closed path in D, or equivalently $\nabla \times \boldsymbol{v} = 0$ everywhere in D [Ref. 13: pp. 369-376].

From the above theorem, coupled with Eq.(10), it is clear that the necessary and sufficient condition for the value of the line integral in expression (12) to be independent of the path C is that

$$\frac{\partial v_2}{\partial z} = \frac{\partial v_3}{\partial y}, \qquad \frac{\partial v_3}{\partial x} = \frac{\partial v_1}{\partial z}, \qquad \frac{\partial v_1}{\partial y} = \frac{\partial v_2}{\partial x} \tag{13}$$

B. THE SURFACE INTEGRAL ALGORITHM

In Chapter I.D., a conceptual overview of the surface integral approach to the motion planning of nonholonomic systems was presented. With the mathematical details necessary for a complete understanding of the algorithm now covered, a more detailed treatment of the method is in order. It should be noted that the algorithm is best illustrated through the use of appropriate examples. This will be the subject of Chapter III. At this point however, it is well worth the effort to discuss the theoretical and mathematical basis of the algorithm.

Consider now a nonholonomic system where one of the dependent variables is p and is constrained by the nonholonomic differential expression

$$dp = v_1 dx + v_2 dy \tag{14}$$

where x and y are taken to be the independent variables and v_1 and v_2 are general functions of x and y.

If an attempt is made to integrate Eq.(14) along some closed curve C in x-y space

$$\oint_C dp = \oint_C (v_1 dx + v_2 dy) \tag{15}$$

it is clear that the attempt would be a failure since nonholonomic constraints are, by definition, nonintegrable. However, since the expression on the right hand side of

Eq.(14) is not integrable, it is therefore not exact. It follows then, from the discussion on the path independence of line integrals, that *if* such a curve C could be found and the integration performed, the resulting change in p would be dependent on the nature of C. In other words, the evolution of the dependent variable p as the independent variables x and y traverse a closed loop path in x-y space is entirely dependent on the shape of that path. It seems then, that a desired change in the value of the dependent variable p could be affected by choosing an appropriate path C in x-y space about which the independent variables x and y traverse. The obvious question is how might this path be chosen given the nonintegrable nature of Eq.(15).

At this point, Stoke's Theorem comes to the rescue. Suppose the desired change in p is given by Δp. Then, using Stoke's Theorem (in the simplified form of Green's Theorem), Eq.(15) can be recast into the following form:

$$\oint_C dp = \oint_C (v_1 dx + v_2 dy) = \int\int_S \left(\frac{\partial v_2}{\partial x} - \frac{\partial v_1}{\partial y} \right) dx dy = \Delta p \qquad (16a)$$

If the double integral of Eq.(16a) can be evaluated, then the problem of determining the appropriate closed curve C is reduced to finding a surface area S in which the curve C is defined by the outline of this surface area. The integration problem can be simplified by choosing this surface area to be rectangular in shape with sides parallel to the x and y axis. Placing limits on the double integral of Eq.(16a) results in

$$\Delta p = \int_{y_l}^{y_u} \int_{x_l}^{x_u} \left(\frac{\partial v_2}{\partial x} - \frac{\partial v_1}{\partial y} \right) dx dy \qquad (16b)$$

where x_l and x_u represent the lower and upper limits of the rectangle along the x axis and y_l and y_u represent the lower and upper limits of the rectangle along the y axis. A simple way of solving this problem thus involves performing the double integration dictated by Eq.(16b), choosing three of the four required limits based on the physical considerations of the problem, and solving the resulting algebraic

expression for the fourth and final limit. With this information in hand, the closed curve C can be constructed and the independent variables x and y caused to traverse around it to produce the desired change in p. As stated in Chapter I.D., the complete surface integral algorithm involves first moving the independent variables to their desired values noting the resulting final values of the dependent variables and then calculating an appropriate closed loop path in the space of the independent variables, using the method described above, such that the desired change in the values of the dependent variables is brought about.

This is the surface integral algorithm for planning the motion of nonholonomic systems. Its utility and ease of implementation is demonstrated via the examples to be discussed in Chapter III. Before proceeding to those examples however, it is worth noting some of the more salient features of the algorithm.

C. NOTES ON THE VERSATILITY OF THE SURFACE INTEGRAL ALGORITHM

The surface integral algorithm provides a simple and effective means of determining the trajectories required to drive all of the configuration variables of a nonholonomic mechanical system to their desired values. The following features of the algorithm make it particularly attractive.

1. Location of the Closed Trajectory in the Space of the Independent Variables

Once again, consider a nonholonomic system where one of the dependent variables is p and is constrained by the nonholonomic differential expression

$$dp = v_1 dx + v_2 dy + v_3 dz \tag{17}$$

where x, y, and z are taken to be the independent variables and v_1, v_2, and v_3 are general functions of x, y, and z. Assume now that there exists some closed trajectory C of

the independent variables x, y, and z that produces a change in the dependent variable p by some desired amount Δp. If (x_0, y_0, z_0) is any point on this closed trajectory, and if the initial configuration of the system is (x_0, y_0, z_0, p_0), then after the system moves along C once, its configuration will be $(x_0, y_0, z_0, p_0 + \Delta p)$. Refer to Fig.4(a). If the closed curve C was traversed in the opposite direction, then the final configuration of the system would have been $(x_0, y_0, z_0, p_0 - \Delta p)$. Now consider the initial configuration of the system to be (x', y', z', p_0) such that (x', y', z') does not lie on C. Let P be any path segment connecting the point (x', y', z') and a point (x_0, y_0, z_0) on the closed curve C. Refer to Fig.4(b). Let δp denote the change in the dependent variable p as x, y, and z move along the path segment P from (x', y', z') to (x_0, y_0, z_0). Then, if the system moves from the initial configuration (x', y', z', p_0) to the closed curve C, traverses the closed curve C once, and finally retraces the path segment P backwards, the configuration of the system at the end of the path will be $(x', y', z', p_0 + \Delta p)$. This is true because the surface integral of the area bounded by the closed curve beginning and ending at the point (x', y', z') is equal to the surface integral of the area bounded by the closed curve C. From this discussion, it follows that the closed curve C that can bring about the desired change in the dependent variable can lie anywhere in the space defined by the independent generalized coordinates - it does not have to pass through the initial configuration of the system. This feature of the surface integral algorithm is extremely useful and will prove its worth in the example systems to be dicussed in Chapter III.

2. Motion Planning in the Presence of Additional Constraints

Often times, mechanical systems are subjected to constraints of motion over and above those arising from the choice of coordinates. Obstacles in the workspace provide the most salient example. The rolling disk of Figs.1(b) and 2(a) for instance, might have its allowed motion restricted by a wall or similar obstacle. The motions

of a robot on an automobile assembly line must be planned so as to avoid inadvertent contact with the cars it is operating on. In order to be effective, a motion planning algorithm must allow for the generation of admissible trajectories in the presence of additional constraints. With regard to nonholonomic systems, the surface integral algorithm provides just such a capability. This capability will be demonstrated in the examples of Chapter III.

3. Algorithmic Singularity

Virtually all motion planning algorithms, when applied to any given mechanical system, entail the possibility of mathematical singularity. An effective algorithm must provide a means for coping with this problem when it arises. In Chapter III., the ability of the surface integral algorithm to deal with mathematical singularity will be readily apparent.

4. Reachability

The reachability of a given mechanical system can best be defined as its ability to arrive at any desired configuration from any other. Obviously, the reachability of a system is an important consideration. Implementation of the surface integral algorithm provides a means of ascertaining the reachability of a nonholonomic system. In Chapter III., the general method of determining the reachability of a nonholonomic system will be discused and the method demonstrated via the examples of that chapter.

5. Repeatability

The basis of the surface integral algorithm derives from the fact that closed trajectories of the independent variables result in a change in the values of the dependent variables. In particular situations however, it may be desirable to find closed trajectories of the independent variables that result in no net change of the dependent variables. Motion of this type is termed repeatable motion due to the fact that all of

the coordinate variables return to their original values upon completion of the motion. Robots programmed to perform repetitive tasks (such as automobile welding) for example, must be capable of repeatable motion in order to perform the same task over and over again. While the issue of repeatability is theoretically trivial in the case of holonomic systems, such is not the case for nonholonomic systems. In Chapter III., it will be demonstrated that the trajectories needed to produce repeatable motion in a nonholonomic mechanical system can be generated easily through application of the surface integral algorithm.

Thus far, this paper has presented a description of nonholonomic mechanical systems and the nonholonomic motion planning problem, the mathematical basis of the surface integral algorithm for solving the nonholonomic motion planning problem, and a discussion of the surface integral algorithm itself. Additionally, the various attractive features of the algorithm have been briefly described. In the next chapter, the algorithm will be applied to two simple nonholonomic systems: a two dimensional free flying space robot and the rolling disk of Figs.1(b) and 2(a). These two examples will demonstrate the exceptional utility, simplicity, and versatility of the surface integral algorithm.

III. APPLIED EXAMPLES OF THE SURFACE INTEGRAL ALGORITHM

A. THE PLANAR SPACE ROBOT

In this part of Chapter III., the surface integral algorithm for the motion planning of nonholonomic systems will be illustrated through the example of a free flying, two dimensional space robot. The robot consists of two links mounted on a space vehicle as shown in Fig.5. Such a system can be described by five coordinates: x_0, y_0, and θ_0 representing the position of the center of mass and the orientation of the space vehicle, and θ_1 and θ_2 representing the joint angles of the manipulator. The requirement that the linear momentum of the system be conserved leads to two holonomic constraints of motion while angular momentum conservation leads to one nonholonomic constraint. Because the system is described by five coordinates and three equations of constraint, the planar space robot possesses two degrees of freedom.

The holonomic constraints that arise due to the conservation of linear momentum allow for the elimination of the variables x_0 and y_0 from the kinematic equations describing the system. The nonholonomic constraint however, does not allow for the elimination of any of the variables due to the fact that it consists of a nonintegrable relationship between the derivatives of the remaining coordinates, namely $\dot{\theta}_0$, $\dot{\theta}_1$, and $\dot{\theta}_2$. The entire system is therefore completely described by three generalized coordinates $(\theta_0, \theta_1, \theta_2)$ and one nonholonomic constraint equation due to the conservation of angular momentum. With some effort, this nonholonomic constraint equation can be derived and is found to be given by the relation

$$\dot{\theta}_o = \frac{1}{\Delta}\left(a\dot{\theta}_1 + b\dot{\theta}_2\right) \tag{18}$$

where,

$$\Delta \triangleq (\frac{1}{2}m_1 + m_2)^2 l_1^2 + \frac{1}{4}m_2^2 l_2^2 - (m_0 + \frac{1}{2}m_1)m_2 l_1 l_2 \cos\theta_2 - M\left(I + (\frac{1}{4}m_1 + m_2)l_1^2 + \frac{1}{4}m_2 l_2^2\right)$$

$$a \triangleq -\Delta - M I_0$$

$$b \triangleq M\left(I_2 + \frac{1}{4}m_2 l_2^2 + \frac{1}{2}m_2 l_1 l_2 \cos\theta_2\right) - \frac{1}{4}m_2^2 l_2^2 - \frac{1}{2}m_2(\frac{1}{2}m_1 + m_2)l_1 l_2 \cos\theta_2 \qquad (19)$$

and where m_0, m_1 and m_2 are the masses of the space vehicle and the two links; I_0, I_1 and I_2 are the moments of inertia of the space vehicle and the two links about their center of masses; l_1 and l_2 are the length of the two links; and $M = (m_0 + m_1 + m_2)$ and $I = (I_0 + I_1 + I_2)$.

The physical effect of the nonholonomic constraint described by Eq.(18) is that the orientation of the space vehicle, θ_0, drifts when the joints are activated. Because the amount of drift is directly dependent on the motion of the joints, θ_0 is the dependent variable in the system. The nonholonomic motion planning task is therefore to develop trajectories of the independent variables θ_1 and θ_2 which drive the entire system to some desired configuration. In accordance with the procedure described in Chapter II.B., this will be accomplished by first converging the joint angles to their desired values. The orientation of the vehicle will then be converged by executing closed trajectories of the joints. These closed trajectories will be planned using Stoke's Theorem.

Let the arbitrary initial and desired configurations of the robot be denoted by $(\theta_{0i}, \theta_{1i}, \theta_{2i})$ and $(\theta_{0f}, \theta_{1f}, \theta_{2f})$ respectively. Upon initial convergence of the independent variables θ_{1i} and θ_{2i} to their desired values θ_{1f} and θ_{2f}, let the orientation of the space vehicle drift from θ_{0i} to some intermediate value θ_{0d}. The task then is to use Stoke's Theorem to plan a cyclic motion for the joints of the manipulator such that the orientation of the space vehicle changes from θ_{0d} to θ_{0f} while the joint angles come

back to their desired configuration. Rewriting Eq.(18) in differential form yields

$$d\theta_0 = \frac{1}{\Delta}\left(a\, d\theta_1 + b\, d\theta_2\right) \tag{20}$$

Integrating Eq.(20) about a closed curve C in the θ_1-θ_2 plane and applying Stoke's Theorem in the form given by Eq.(11) yields

$$\theta_{0f} - \theta_{0d} = \oint d\theta_0 = \oint_C \left(\frac{a}{\Delta}d\theta_1 + \frac{b}{\Delta}d\theta_2\right) = \iint_S \left[\frac{\partial}{\partial\theta_1}(\frac{b}{\Delta}) - \frac{\partial}{\partial\theta_2}(\frac{a}{\Delta})\right] d\theta_1 d\theta_2 \tag{21}$$

where S is the surface in the θ_1-θ_2 plane confined within the closed curve C. Substitution of the expressions for a, b, and Δ from Eq.(19) and specification of the surface S as a rectangle with sides parallel to the θ_1 and θ_2 axis leads to

$$(\theta_{0f} - \theta_{0d}) = MI_0 \int_{\theta_{2l}}^{\theta_{2u}} \int_{\theta_{1l}}^{\theta_{1u}} \frac{\partial}{\partial\theta_2}\left(\frac{1}{A + B\cos\theta_2}\right) d\theta_1 d\theta_2 \tag{22}$$

where

$$\begin{aligned} A &\triangleq (\frac{1}{2}m_1 + m_2)^2 l_1^2 + \frac{1}{4}m_2^2 l_2^2 - M\left(I + (\frac{1}{4}m_1 + m_2)l_1^2 + \frac{1}{4}m_2 l_2^2\right) \\ B &\triangleq -(m_0 + \frac{1}{2}m_1)m_2 l_1 l_2 \end{aligned} \tag{23}$$

and where θ_{1l} and θ_{1u} denote the lower and upper extremities of θ_1 in the rectangular path while θ_{2l} and θ_{2u} denote the same for θ_2. Finally, performing the combined differentiation and integration dictated by Eq.(22) yields

$$\frac{\overline{\theta}_0}{n} = M\, I_0\, (\theta_{1u} - \theta_{1l})\left[\frac{1}{A + B\cos\theta_{2u}} - \frac{1}{A + B\cos\theta_{2l}}\right] \tag{24}$$

where

$$\overline{\theta}_0 = \theta_{0f} - \theta_{0d}$$

and n equals the desired number of cyclic motions about the closed loop trajectory.

Clearly, for a desired change in θ_0 (given by $\overline{\theta}_0$), an appropriate closed loop trajectory of the joint variables θ_1 and θ_2 can be constructed simply by specifying the

trajectory to be rectangular in shape and choosing values of θ_{1l}, θ_{1u}, θ_{2l}, and θ_{2u} such that Eq.(24) is satisfied.

To illustrate, consider a robot with the following kinematic and dynamic parameters: $m_0 = 27.44$ kg, $m_1 = 5.38$ kg, $m_2 = 2.64$ kg, $I_0 = 1.520$ kgm^2, $I_1 = 0.115$ kgm^2, $I_2 = 0.028$ kgm^2, $l_1 = 0.50$ m, and $l_2 = 0.35$ m. Let the initial configuration of the system be $(\theta_{0i}, \theta_{1i}, \theta_{2i}) = (0.0, 15.0, 15.0)$ degrees and the final desired configuration be $(\theta_{0f}, \theta_{1f}, \theta_{2f}) = (-20.0, 45.0, 0.0)$ degrees. Furthermore, specify that the desired change in the dependent variable θ_0 occur only after three complete cycles of the closed loop trajectory. Using computer simulation, the independent variables θ_1 and θ_2 are first converged from their current values to their desired values by following the straight line trajectory OA shown in Fig.6(a). During this process, the orientation of the space vehicle drifts from $\theta_{0i} = 0.0$ degrees to $\theta_{0d} = -12.87$ degrees as shown in Fig.6(b). Thus, $\overline{\theta}_0 = \theta_{0f} - \theta_{0d} = -7.13$ degrees. If a cyclic motion of the joints is to be planned such that after three complete cycles the orientation of the space vehicle changes by the desired amount, then for each cycle the required change of orientation would be $\overline{\theta}_0/n = -7.13/3.0 = -2.38$ degrees. Choosing $\theta_{1l} = 45.0$ degrees and $\theta_{2l} = 0.0$ degrees to correspond with point A of Fig.6(a) and arbitrarily choosing $\theta_{1u} = 125.0$ degrees results in $\theta_{2u} = 53.4$ degrees, calculated using Eq.(24). Note that all angles must be converted from degrees to radians prior to using Eq.(24).

The values $(\theta_{1l}, \theta_{1u}, \theta_{2l}, \theta_{2u}) = (45.0, 125.0, 0.0, 53.4)$ degrees define a rectangular path $ABCDA$ in the θ_1-θ_2 plane, shown in Fig.6(a), which, when traversed three times by the robot joints, will cause the dependent variable θ_0 to converge to its desired value. The evolution of all the configuration variables for the path $OABCDA$ when the closed trajectory $ABCDA$ is traversed three times is shown in Fig.6(b). Note that all of the configuration variables do in fact converge to their desired values.

The above example confirms the validity of the surface integral algorithm. It is now worth the effort to illustrate some of the more versatile features of the algorithm in the context of this example.

In Chapter II.C.2., it was noted that motion planning must often occur in the presence of additional constraints. Suppose now that a situation exists such that the following joint limit is imposed on the space robot: $|\theta_1| \leq 90$ degrees. Clearly, the closed trajectory *ABCDA* is no longer feasible since it requires θ_1 to come to a maximum value of $\theta_{1u} = 125.0$ degrees. Since this value was chosen arbitrarily to begin with, there is complete liberty to respecify it as, say, $\theta_{1u} = 75.0$ degrees. Taking θ_{1l} and θ_{2l} to have the same values as before, maintaining the requirement that three complete cycles of the closed loop trajectory be executed, and recalculating the value of θ_{2u} using Eq.(24) yields $\theta_{2u} = 89.2$ degrees. The values $(\theta_{1l}, \theta_{1u}, \theta_{2l}, \theta_{2u}) = (45.0, 75.0, 0.0, 89.2)$ degrees define a revised rectangular path *AEFGA* shown in Fig.7(a) which, when traversed three times by the robot joints, will cause the dependent variable θ_0 to converge to its desired value subject to the constraint $|\theta_1| \leq 90$ degrees. The evolution of all the configuration variables for the path *OAEFGA* when the closed trajectory *AEFGA* is traversed three times is shown in Fig.7(b).

Now suppose yet another constraint is imposed, namely $|\theta_2| \leq 80$ degrees. This constraint now renders both the paths *ABCDA* and *AEFGA* infeasible. To obtain a feasible path, one might choose to respecify θ_{1u} once again in order to obtain a suitable value for θ_{2u}. However, there is another way. If the requirement to execute three cycles of the closed trajectory is lifted, one would have the freedom to choose any number of cycles. Choosing the number of cycles to be $n = 6$ and maintaining $(\theta_{1l}, \theta_{1u}, \theta_{2l}) = (45.0, 75.0, 0.0)$ degrees yields $\theta_{2u} = 61.86$ degrees. These values now define the path *AHIJA* shown in Fig.8(a) which, when traversed six times, will converge

the dependent variable θ_0 subject to the constraints $|\theta_1| \leq 90$ degrees and $|\theta_2| \leq 80$ degrees. The evolution of the configuration variables for the path $OAHIJA$ is shown in Fig.8(b).

The above examples illustrate that using the surface integral algorithm to plan the closed trajectory of the independent variables needed to converge the dependent variable in the presence of additional constraints is a relatively trivial problem. One need only choose an appropriate value of θ_{1u} or an appropriate number of cyclic motions of the joints. This feature of the surface integral algorithm is extremely powerful and gives it a distinct advantage over other nonholonomic motion planning algorithms.

Another attractive feature of the surface integral algorithm that can be demonstrated using the two dimensional space robot is its ability to prove the reachability of specific nonholonomic systems. The reachability of the space robot can be proven by showing that there exists a rectangular surface in the θ_1-θ_2 plane defined by the points $(\theta_{1l}, \theta_{1u}, \theta_{2l}, \theta_{2u})$ such that the equality in Eq.(22) can be satisfied for any arbitrary value of $\bar{\theta}_0 = \theta_{0f} - \theta_{0d}$. Note that the initial values of θ_1 and θ_2 do not necessarily have to lie on the boundary of the rectangular surface. This follows from the discussion of Chapter II.C.1. Also note that if the identity in Eq.(22) can be satisfied for some value of $\bar{\theta}_0$ by travelling along the boundary of the rectangle in the positive direction, then the same identity can be satisfied for $-\bar{\theta}_0$ simply by travelling along the boundary in the negative direction. Finally, if the identity can be satisfied for some value of $\bar{\theta}_0$ by travelling once along the boundary of the rectangle, then the identity can be satisfied for the value $n\bar{\theta}_0$, $n = 1, 2, \cdots$, by travelling n times along the boundary in the same direction. Clearly, the reachability problem thus reduces to showing that the identity in Eq.(22) can be satisfied for any value of $\bar{\theta}_0 \in [0, \epsilon)$ where ϵ is some small positive number. Consider the following quantity from Eq.(24):

$$\alpha \triangleq \left(\frac{1}{A + B\cos\theta_{2u}} - \frac{1}{A + B\cos\theta_{2l}} \right) \tag{25}$$

If θ_{2u} and θ_{2l} are chosen in such a manner so as to ensure that α does not equal zero, Eq.(24) can be rewritten as follows:

$$\frac{\bar{\theta}_0}{M I_0 n \alpha} = \theta_{1u} - \theta_{1l} \tag{26}$$

With this formulation, it is quite obvious that $(\theta_{1u} - \theta_{1l})$ can be chosen such that Eq.(26) is satisfied thus proving that Eq.(22) can be satisfied for any value of $\bar{\theta}_0 \in [0, \epsilon)$.

A final feature of the surface integral algorithm that can best be illustrated with the space robot concerns the problem of repeatability. In Chapter II.C.5., it was stated that the surface integral algorithm allowed for the calculation of trajectories needed to produce repeatable motion. In particular situations, a space robot may be expected to perform a repetitive task. In such a situation, the end effector of the robot as well as its configuration variables will all have to move along closed trajectories. If the joints of the robot shown in Fig.5 move along closed trajectories, the dependent variables x_0 and y_0 will always move along closed trajectories because of the holonomic nature of the linear momentum constraints. The dependent variable θ_0 will however not move along a closed trajectory in the general case. If the net change in θ_0 were also to be zero as the joints moved along a closed rectangular path, then from Eq.(24) the necessary conditions that would have to be satisfied are $\theta_{1u} = \theta_{1l}$ or $\cos\theta_{2u} = \cos\theta_{2l}$. The first condition leads to the trivial case where the first joint of the robot will have to be kept fixed. The second condition states that repeatability is assured as long as $\theta_{2u} + \theta_{2l} = 2n\pi$, $n = 0, \pm1, \pm2, \cdots$. The examples considered thus far demonstrate that a significant amount of flexibility exists with regard to choosing the closed trajectories. Although the condition $\theta_{2u} + \theta_{2l} = 2n\pi$, $n = 0, \pm1, \pm2, \cdots$ will greatly

restrict the available trajectories, it will still be possible to choose from a variety of paths that will produce repeatable motion.

To illustrate this point, consider the initial configuration of the robot to again be $(\theta_{0_i}, \theta_{1_i}, \theta_{2_i}) = (0.0, 15.0, 15.0)$ degrees. This time however, the task is to move the joints from their initial configuration to some desired configuration and back to their initial configuration without effecting any change in the value of θ_0. Again choosing a rectangular trajectory for the joint variables and substituting the condition that $\theta_{2u} + \theta_{2l} = 2\pi$ (letting $n = 1$), recasts Eq.(24) into the following form:

$$0 = M\, I_0\, (\theta_{1u} - \theta_{1l}) \left[\frac{1}{A + B\cos\theta_{2u}} - \frac{1}{A + B\cos(2\pi - \theta_{2u})} \right] \tag{27}$$

If the desired configuration of the joints is given by $(\theta_{1f}, \theta_{2f}) = (60.0, 30.0)$ degrees, and $(\theta_{1u}, \theta_{2u})$ are chosen to be $(60.0, 30.0)$ degrees, then θ_{2l} is calculated to be $2\pi - 30.0 = 330.0 = -30.0$ degrees. Choosing θ_{1l} to be 15.0 degrees so that the initial configuration of the system lies on the planned closed loop path results in the trajectory $OAKLMO$ shown in Fig.9(a). Assume now that the joints must perform the required task five times, each time moving from point O to point L and back again to O. The evolution of all the configuration variables as this is accomplished over the path $OAKLMO$ is shown in Fig.9(b). Note that the motion is completely repeatable. All of the configuration variables, including the vehicle orientation θ_0, return to their initial values following each execution of the closed trajectory $OAKLMO$.

In this first part of Chapter III., the surface integral algorithm was applied to the motion planning of a planar space robot. The example illustrated the validity of the algorithm as well as its ability to handle additional motion constraints. The example also demonstrated how the algorithm can be used to ascertain a particular system's reachability. Finally, the algorithm was used to plan trajectories which result in repeatable motion of all the coordinates. In Chapter III.B., the algorithm will be

applied to yet another nonholonomic system, the rolling disk. This example will demonstrate the algorithm's ability to avoid cases of singularity and will prove that the closed trajectory needed to converge the dependent variables can lie anywhere in the space of the independent variables.

B. THE ROLLING DISK

In this part of Chapter III., the surface integral algorithm will be applied to the motion planning of the rolling disk first mentioned in Chapter I.A.. This example will serve to further illustrate the algorithm itself as well as the algorithm's ability to handle cases of algorithmic singularity.

As discussed previously, the configuration of the rolling disk of Figs.1(b) and (2) can be described by the coordinates (x, y, θ, α) and the differential motion constraints

$$dx = r \sin\alpha \; d\theta \tag{28a}$$

$$dy = r \cos\alpha \; d\theta \tag{28b}$$

where x and y represent the dependent variables while θ and α are taken as the independent variables. To plan a path from some initial configuration $(x_i, y_i, \theta_i, \alpha_i)$ to some desired configuration $(x_f, y_f, \theta_f, \alpha_f)$, the surface integral algorithm requires that the independent variables first be converged to their desired values as the dependent variables evolve to some intermediate configuration (x_d, y_d). A closed path in the space of the independent variables is then planned using Stoke's Theorem such that the dependent variables converge from (x_d, y_d) to (x_f, y_f) as the independent variables travel along this closed path. Let C be such a closed path in the θ-α plane. Then the change of the variables x and y as θ and α traverse this path is given by

$$x_f - x_d = \oint_C r \sin\alpha \; d\theta = \int\int_S -r \cos\alpha \; d\theta \; d\alpha \tag{29}$$

$$y_f - y_d = \oint_C r \cos\alpha \; d\theta = \int\int_S r \sin\alpha \; d\theta \; d\alpha \tag{30}$$

where Stoke's Theorem, in the simplified form of Eq.(11), was applied to convert the line integrals into surface integrals. S is therefore the surface in the θ-α plane enclosed by the closed curve C. Specification of this surface as a rectangle with sides parallel to the θ and α axis leads to

$$x_f - x_d = -\int_{\alpha_l}^{\alpha_u}\int_{\theta_l}^{\theta_u} r\cos\alpha \, d\theta \, d\alpha = -r(\theta_u - \theta_l)(\sin\alpha_u - \sin\alpha_l) \tag{31}$$

$$y_f - y_d = \int_{\alpha_l}^{\alpha_u}\int_{\theta_l}^{\theta_u} r\sin\alpha \, d\theta \, d\alpha = -r(\theta_u - \theta_l)(\cos\alpha_u - \cos\alpha_l) \tag{32}$$

where θ_l and θ_u denote the lower and upper extremities of θ in the rectangular path, and α_l and α_u denote the same for α. Eqs.(31) and (32) can be simplified by letting $b = \alpha_u - \alpha_l$ and $a = \theta_u - \theta_l$. With these substitutions, Eqs.(31) and (32) become

$$x_f - x_d = -ra\,[\sin(b + \alpha_l) - \sin\alpha_l] \tag{33}$$

$$y_f - y_d = -ra\,[\cos(b + \alpha_l) - \cos\alpha_l] \tag{34}$$

Simplification through the use of trigonometric identities yields

$$x_f - x_d = -2ra\cos(\alpha_l + \frac{b}{2})\sin\frac{b}{2} \tag{35}$$

$$y_f - y_d = 2ra\sin(\alpha_l + \frac{b}{2})\sin\frac{b}{2} \tag{36}$$

To construct a closed loop path in the θ-α plane that will serve to converge the dependent variables from (x_d, y_d) to (x_f, y_f), one merely needs to choose α_l and solve Eqs.(35) and (36) simultaneously for a and b to obtain

$$b = 2\,[-\alpha_l + \arctan 2\,(y_f - y_d, x_d - x_f)]\,, \qquad 0 < b < 4\pi \tag{37}$$

$$a = \frac{\{(x_f - x_d)^2 + (y_f - y_d)^2\}^{1/2}}{2r\,\sin(b/2)} \tag{38}$$

Since the solutions to the arctan 2 function differ by an angle of 2π, b in Eq.(37) can always be chosen to be a positive number subject to $b < 4\pi$. Furthermore, Eq.(37)

was derived from Eqs.(35) and (36) with the assumption that $a\sin(b/2)$ is a positive number. Thus, in Eq.(38), the positive square root of the numerator on the right hand side is always chosen rather than the negative. This may sometimes lead to negative values of a. In such situations, the path is constructed as though a were positive and then is traversed in the direction opposite to normal convention. A generic closed rectangular path $PQRSP$ with sides of length a and b as well as the required initial path OP needed to converge the independent variables is shown in Fig.10(a). In this figure, α_l has been chosen to be equal to α_f.

At this point, it is worth noting that as the disk moves along the sides QR and SP of the rectangular path $PQRSP$ in Fig.10(a), the value of α must change in the absence of rolling. Since this might be difficult to achieve in practice, such as in the case of a unicyclist, the rectangular path $PQRSP$ can be modified to the path $PQMNP$ shown in Fig.10(b). It is a simple matter to show that the surface integrals in Eqs.(29) and (30) will have the same value for each of these paths. As a result, the path $PQMNP$ produces the same change in the values of the dependent variables x and y as the original path $PQRSP$. The path $PQMNP$ requires α to change only when the disk is rolling and is therefore a more physically feasible path.

Consider now a disk of radius $r = 0.25$ meters at an initial configuration of $(x_i, y_i, \theta_i, \alpha_i) = (0.0, 0.0, 0.0, 0.0)$ meters, degrees. Suppose that the desired configuration of the disk is $(x_f, y_f, \theta_f, \alpha_f) = (1.0, 1.0, 180.0, 30.0)$ meters, degrees. The independent variables θ and α are first converged to their desired values using the straight line path OP shown in Fig.11(a). The values of the dependent variables x and y at the end of this path, obtained via computer simulation, are $x_d = 0.20$ meters and $y_d = 0.75$ meters as shown in Fig.11(b). Choosing a rectangular path with $\alpha_l = \alpha_f = 30.0$ degrees and solving for the values of a and b using Eqs.(37) and (38) results in $a = 130.4$ degrees and $b = 265.3$ degrees. A slight modification to this path using a value of

β = 45.0 degrees in order to allow the value of α to change only while the disk is rolling results in the closed path $PQRSP$, also shown in Fig.11(a). Execution of this path results in the dependent variables evolving from $(x_d, y_d) = (0.20, 0.75)$ meters to $(x_f, y_f) = (1.0, 1.0)$ meters while the independent variables change but finally return to values of $(\theta_f, \alpha_f) = (180.0, 30.0)$ degrees. Fig.11(b) shows the actual path of the disk in the x-y plane.

The above example illustrates the validity of the surface integral algorithm when applied to the rolling disk. However, consider Eq.(38) once again. Note that an algorithmic singularity will occur if $b = 2n\pi$, $n = 0, 1, 2, \cdots$. Substituting this value of b into Eq.(37) reveals that the surface integral algorithm, as discussed thus far, breaks down if α_l, the lower value of α on the requisite closed trajectory, has value

$$\alpha_l = \arctan 2\,(y_f - y_d, x_d - x_f) - n\,\pi, \qquad n = 0, 1, 2, \cdots, \tag{39}$$

As stated in Chapter II.C.3., the surface integral algorithm is equipped to handle such a case. In Chapter II.C.1, it was noted that the closed trajectory of the independent variables needed to converge the dependent variables could lie anywhere in the space of the independent variables. It does not have to pass through any particular configuration of the system. As a result, α_l can be chosen arbitrarily and if by chance that choice results in the equality of Eq.(39) being satisfied, one merely needs to make another choice.

Once again, consider a disk with radius $r = 0.25$ meters and an initial configuration $(x_i, y_i, \theta_i, \alpha_i) = (0.0, 0.0, 0.0, 0.0)$ meters, degrees. This time, let the desired configuration of the disk be $(x_f, y_f, \theta_f, \alpha_f) = (-0.4, 1.0, 180.0, 22.5)$ meters, degrees. As before, the independent variables are first converged to their desired values, this time along the path OT of Fig.12(a). The values of the dependent variables (again obtained via computer simulation) evolve from $(x_i, y_i) = (0.0, 0.0)$ meters to $(x_d, y_d) = (0.15, 0.77)$ meters

as θ and α traverse this path. If α_i were chosen to be equal to α_f as before, Eq. (39) would be very nearly satisfied and the required value of a needed to converge the dependent variables would be inordinately large as evident from Eq.(38). As a result, α_i is not chosen to be equal to α_f but is instead chosen (arbitrarily) as $\alpha_i = 10.0$ degrees. Such a choice results in the current configuration of the system not lying on the closed trajectory needed to converge the dependent variables. The disk must therefore traverse the path segment TU of Fig.12(a) in order to arrive at the start of the requisite closed trajectory. This motion results in the dependent variables evolving from $(x_d, y_d) = (0.15, 0.77)$ meters to $(x'_d, y'_d) = (0.32, 1.33)$ meters. A check of Eq.(39) reveals that with $\alpha_i = 10.0$ degrees, the disk is no longer near a singular configuration. As a result, Eqs.(37) and (38) can now be solved for a and b yielding values of $a = 305.2$ degrees and $b = 26.0$ degrees. Note that the values of x'_d and y'_d were not considered when solving for a and b since the change in the values of the dependent variables $[(x'_d - x_d)$ and $(y'_d - y_d)]$ in traversing the path segment TU will be negated when that same path segment is executed in reverse. The complete closed path $TUVWXUT$, shown in Fig.12(a) and modified as before with a value of $\beta = 45.0$ degrees, results in the convergence of the dependent variables from their intermediate configuration of $(x_d, y_d) = (0.15, 0.77)$ meters to their final desired values of $(x_f, y_f) = (-0.4, 1.0)$ meters. Because the path is closed in the θ-α plane, the independent variables return to their desired values of $(\theta_f, \alpha_f) = (180.0, 22.5)$ degrees. Fig.12(b) shows the actual path of the disk in the x-y plane.

The two rolling disk motion planning problems described above once again demonstrate the validity of the surface integral algorithm. Additionally, in the process of showing that algorithmic singularities can be easily overcome, it was demonstrated that the closed path needed to converge the dependent variables can lie anywhere in the space of the independent variables.

IV. SUMMARY AND RECOMMENDATIONS

In this thesis, an algorithm for calculating the coordinate trajectories required to drive a nonholonomic mechanical system from one point in its configuration space to another has been presented. The algorithm entails first driving the independent variables to their desired values. Closed trajectories of the independent variables are then executed in order to drive the dependent variables to their desired values. Stoke's Theorem is employed to convert the problem of finding an appropriate closed path in the space of the independent variables to one of finding a surface area in that same space such that the dependent variables converge to their desired values as the independent variables traverse along the boundary of this surface area. The algorithm is conceptually simple and applicable to a large class of nonholonomic mechanical systems. The requisite closed trajectories are not restricted to any particular location in the space of the independent variables, the algorithm allows for motion planning in the presence of additional constraints, algorithmic singularities are easily overcome, and questions pertaining to the reachability and repeatability of the system are readily answered. Application of the algorithm to two simple nonholonomic mechanical systems, a planar space robot and a disk rolling without slipping on a flat surface, demonstrate the validity and utility of the algorithm.

The application of this algorithm to other, more practical nonholonomic motion planning problems is a logical next step. An actual three dimensional space structure might be considered. Cyclic motions of the joints of a manipulator attached to the structure could be used to control the attitude of the structure itself. These cyclic motions could be planned using the surface integral approach. This method of controlling the structure would result in significant reductions in cost and weight since

the requirement for fuel consuming thrusters would be minimized. The algorithm might also be applied to the motion planning of a wheeled mobile robot or robotic hand with dextrous fingers. Additionally, it may even prove useful in controlling the orientation of certain underwater vehicles. In summary, the surface integral algorithm provides a new and useful approach to the motion planning of nonholonomic mechanical systems and offers a wide range of possibilities for its implementation.

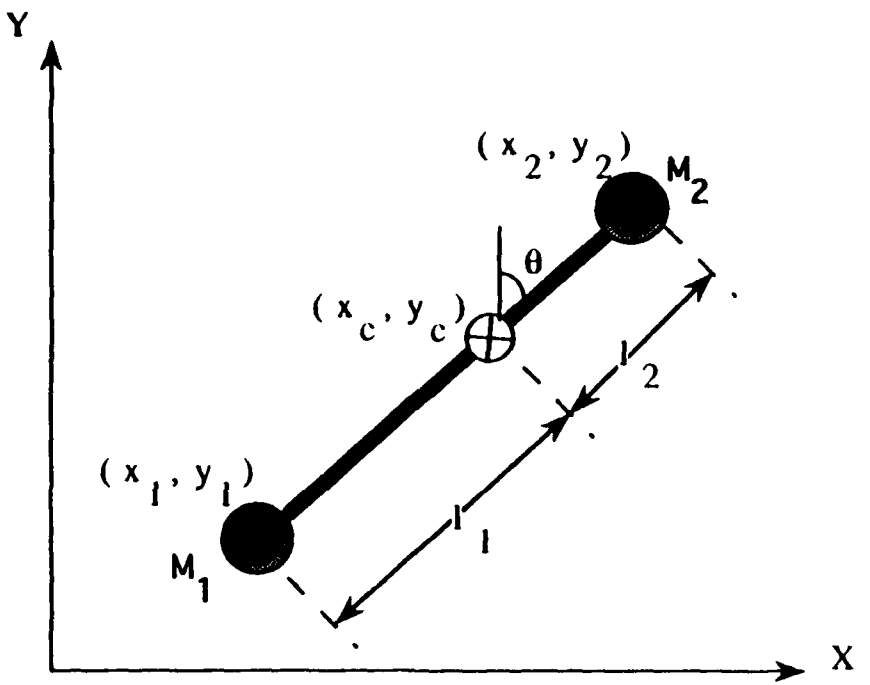

Figure 1(a). A holononic mechanical system consisting of two point masses connected by a thin massless rod. Regardless of the coordinate set chosen to describe the system, the resulting constraints always involve a direct relationship between the coordinates themselves.

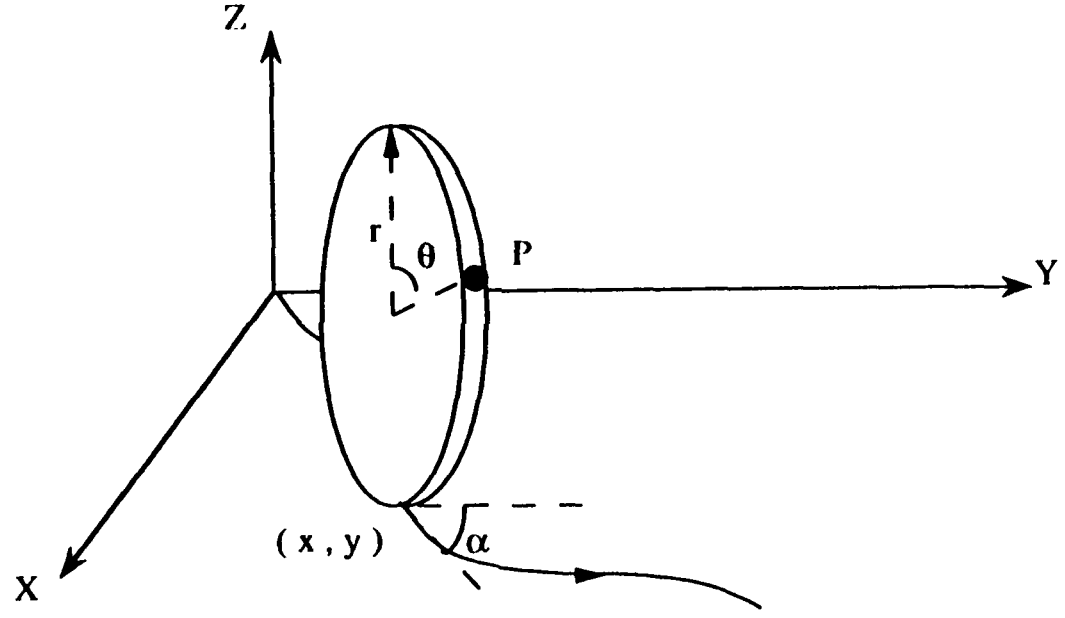

Figure 1(b). A disk rolling without slipping on a flat surface is a nonholonomic mechanical system since the constraints of motion are represented by nonintegrable relationships between the velocities of the system.

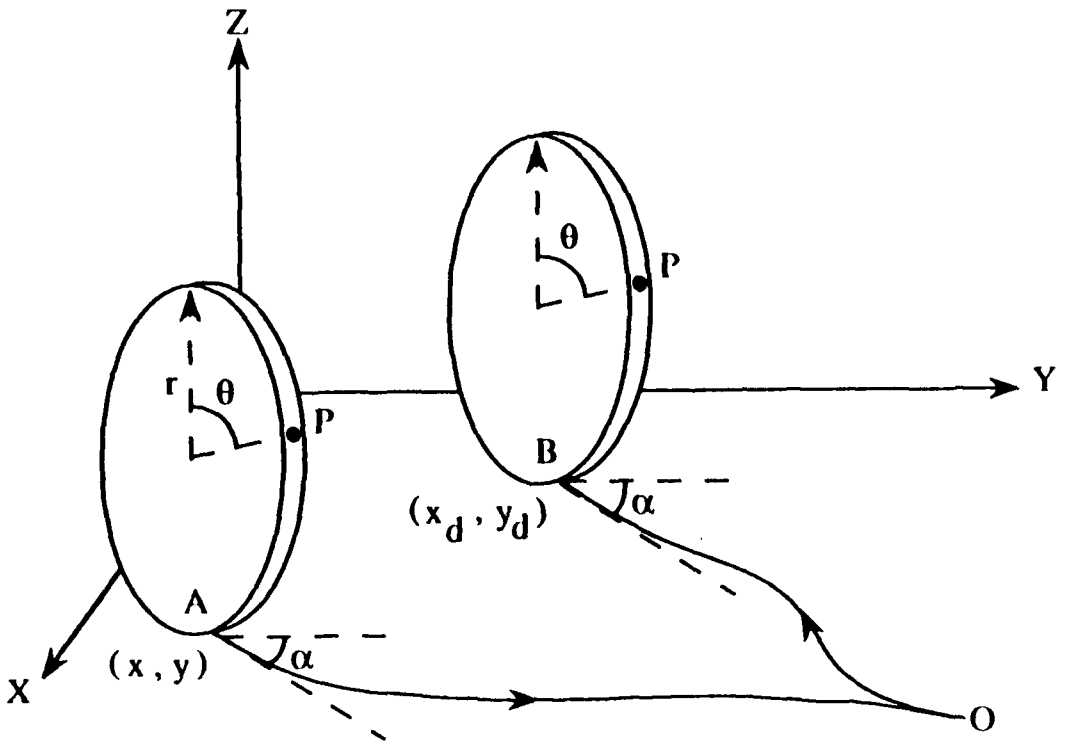

Figure 2(a). The rolling disk can be driven from an initial configuration of (x, y, θ, α) to a desired configuration of $(x_d, y_d, \theta, \alpha)$ by following the path AOB.

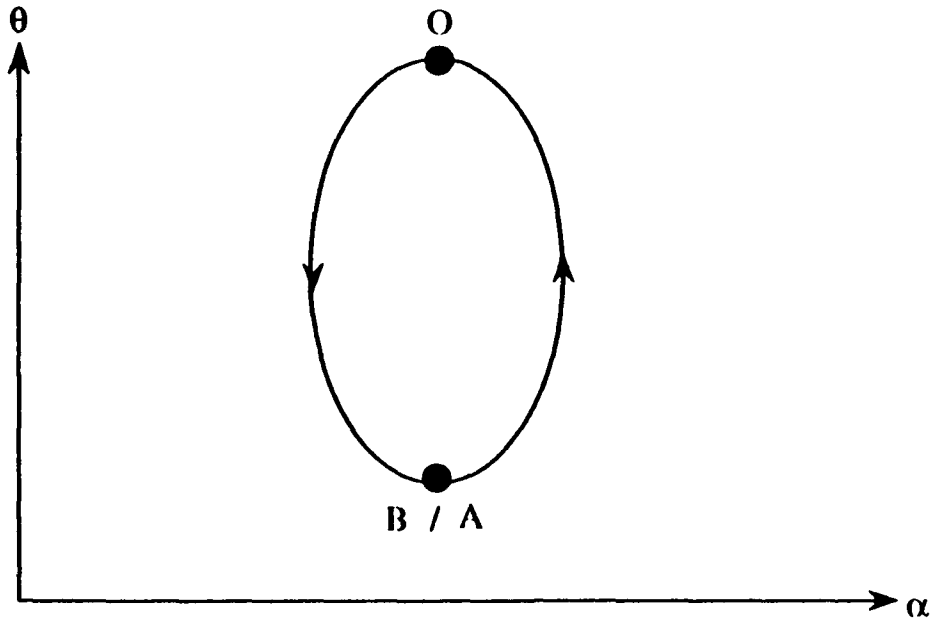

Figure 2(b). The path AOB in x-y-z space shown in figure 2(a) represents a closed loop trajectory in the θ–α plane. Execution of this closed loop trajectory enables the disk to arrive at its desired configuration.

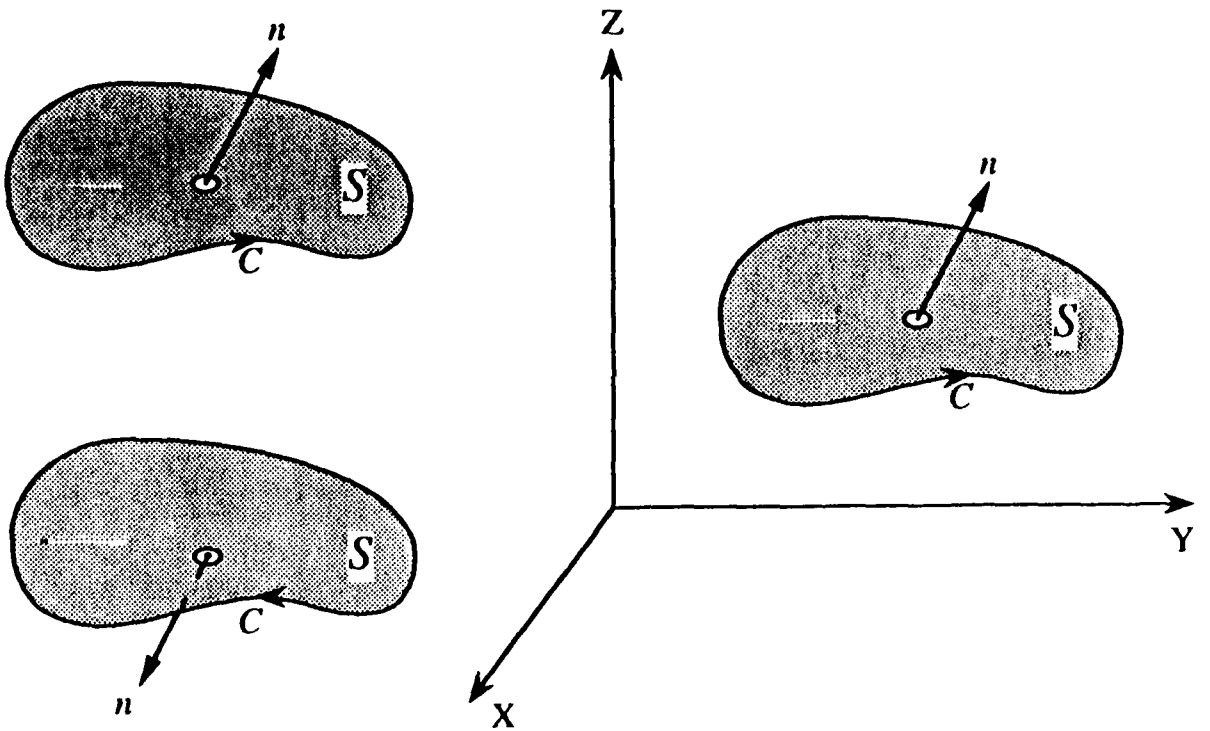

Figure 3 (a). Positive direction of travel along the closed curve C in Stokes Theorem

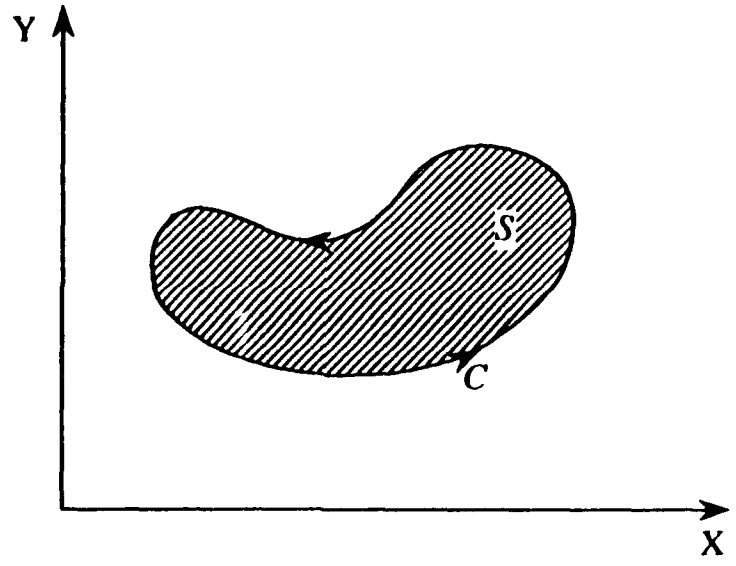

Figure 3 (b). Positive direction of travel along the closed curve C in Green's Theorem

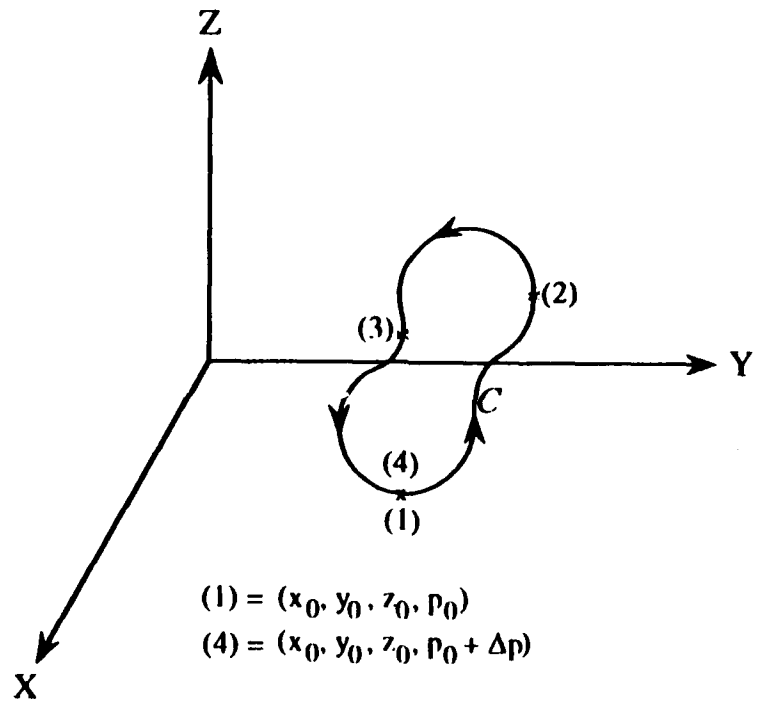

Figure 4 (a). The closed trajectory C in the independent variables x, y, and z produces a change in the dependent variable p by an amount Δp. The initial configuration of the system, (1), lies on this closed trajectory.

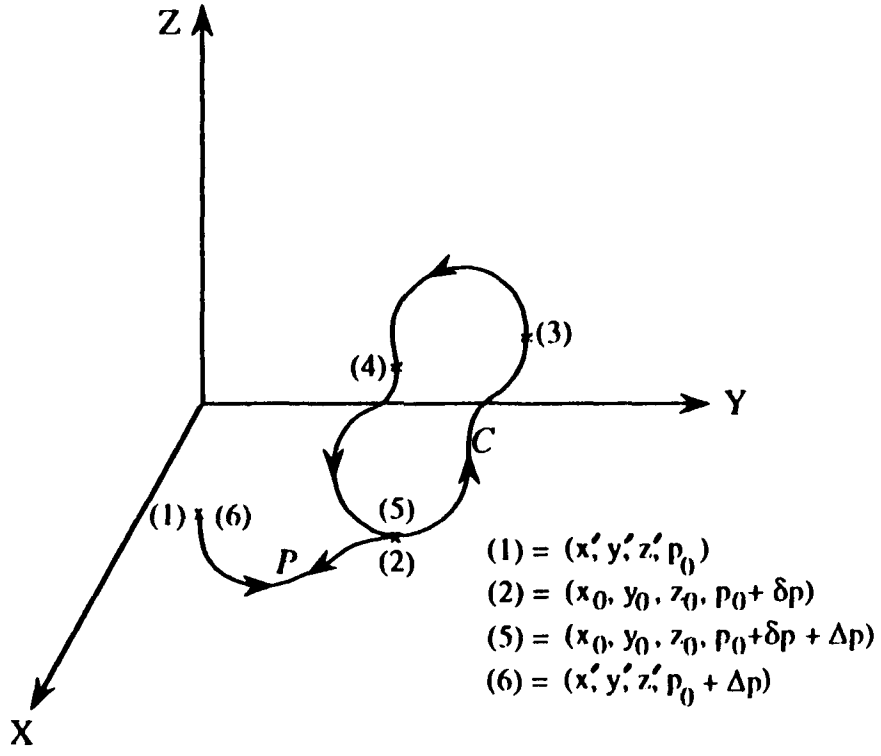

Figure 4 (b). The closed trajectory C in the independent variables x, y, and z produces a change in the dependent variable p by an amount Δp. The initial configuration of the system , (1), does not lie on this closed trajectory.

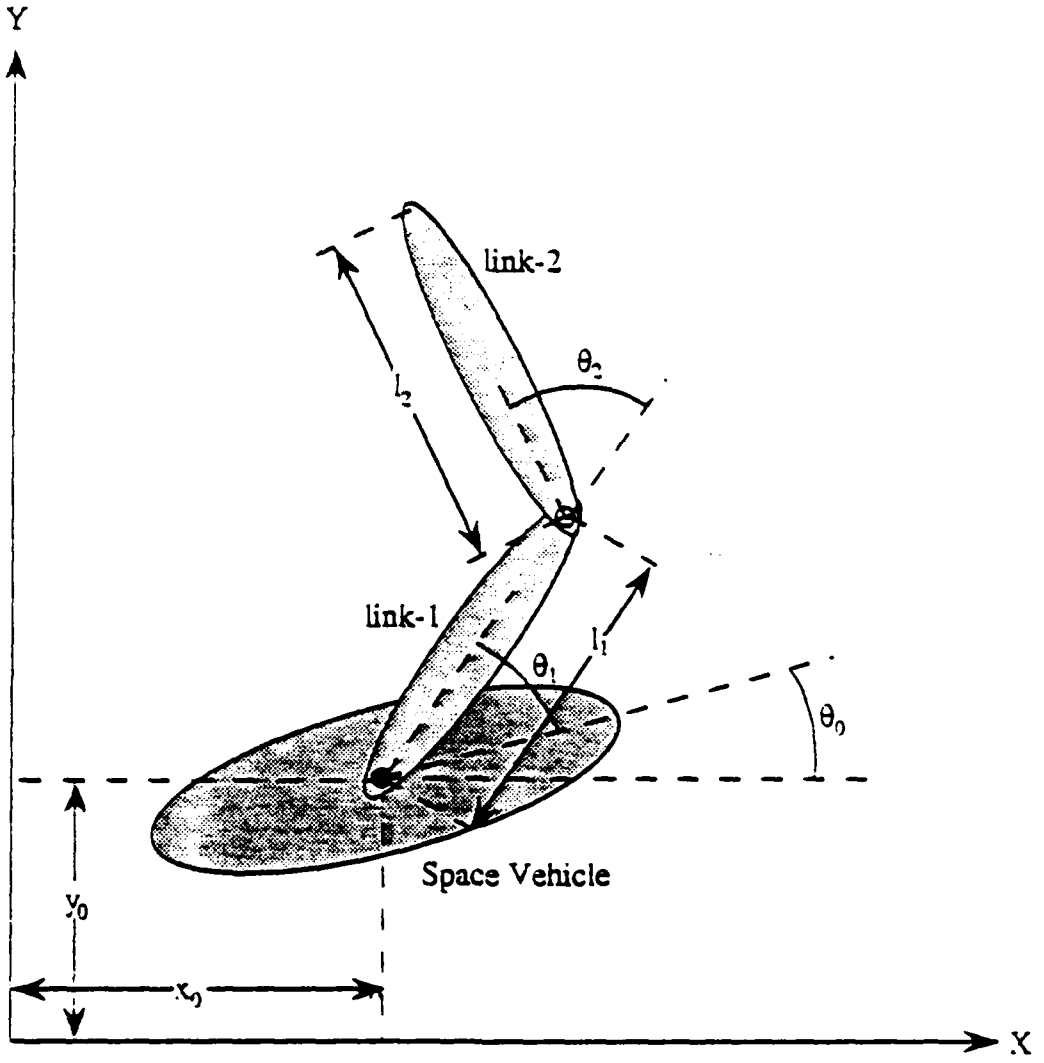

Figure 5. A two-link manipulator mounted on a space vehicle is described by three generalized coordinates: θ_0, θ_1, θ_2. The center of mass of the space vehicle has the coordinates x_0, y_0.

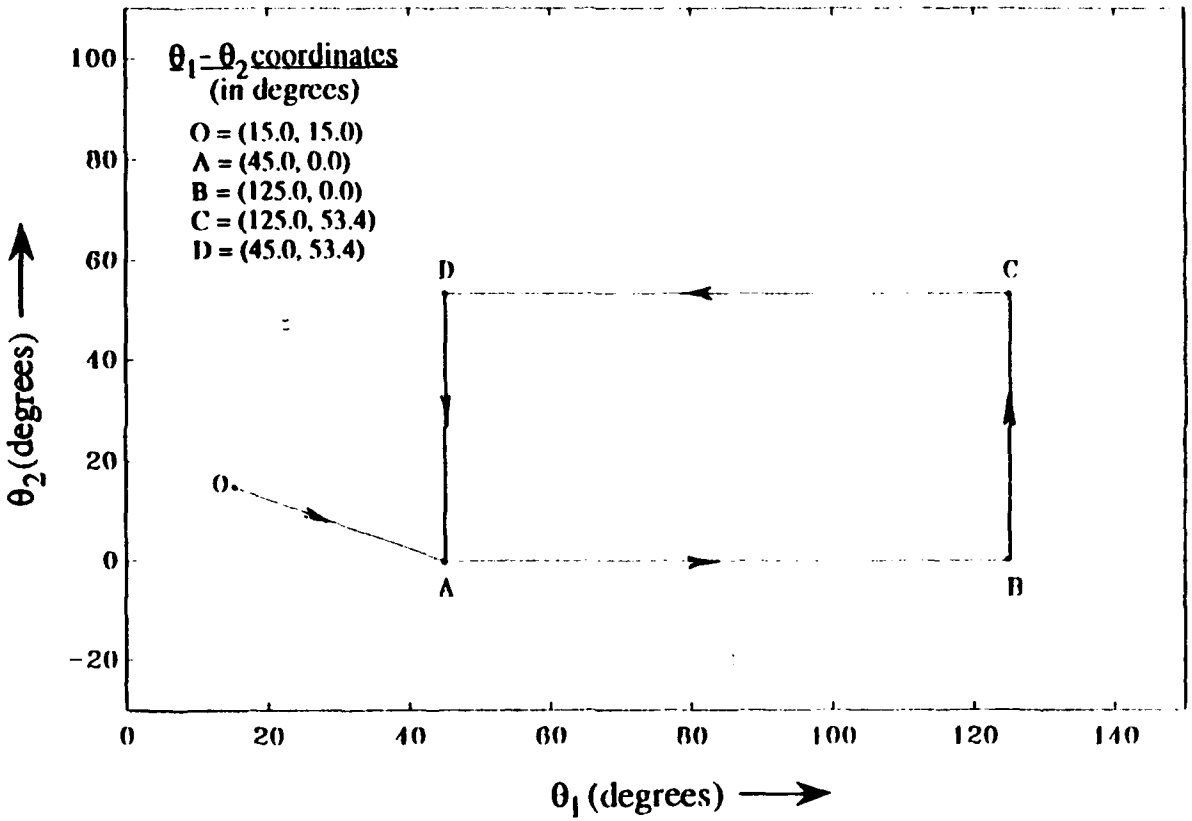

Figure 6(a). The path segment OA followed by the closed trajecory ABCDA converges all of the configuration variables of the space robot to their desired values when the closed trajectory is traversed three times.

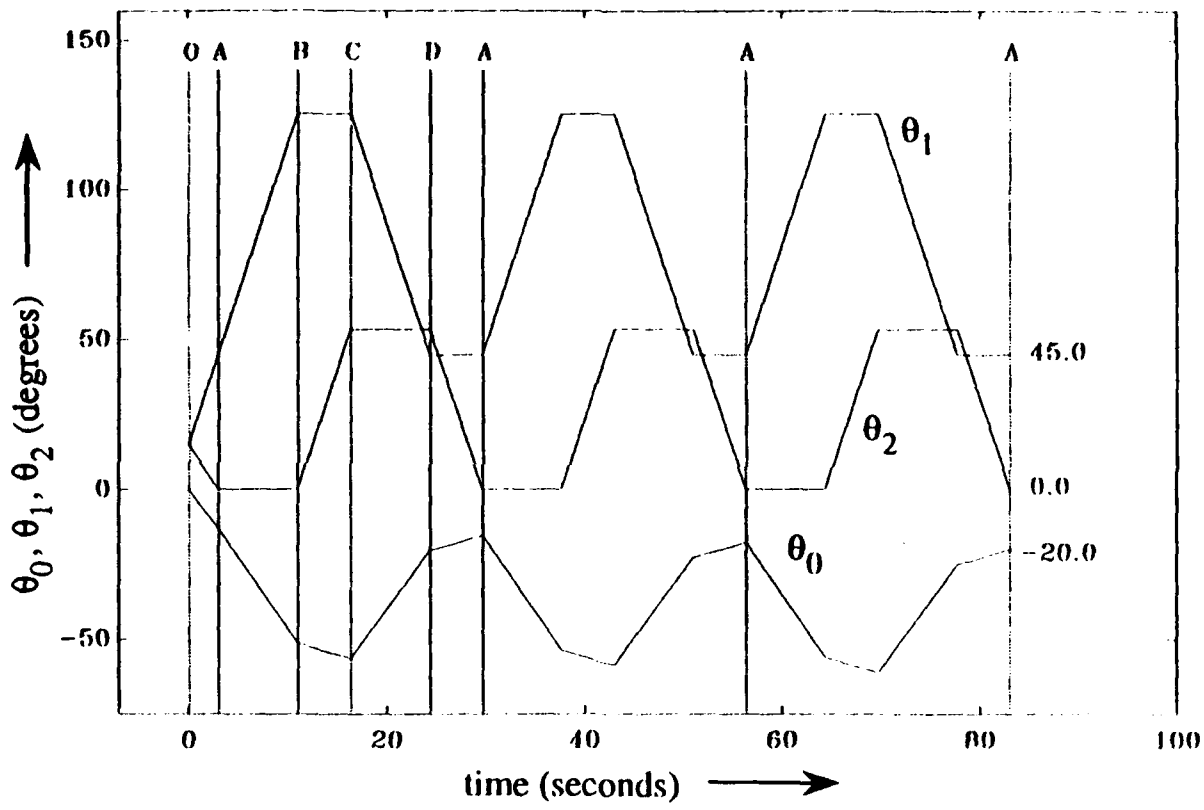

Figure 6(b). Evolution of the configuration variables of the space robot with time when the path segment OA followed by three trips about the closed trajectory ABCDA is executed. Points O, A, B, C, and D in this figure correspond to the same points in figure 6(a).

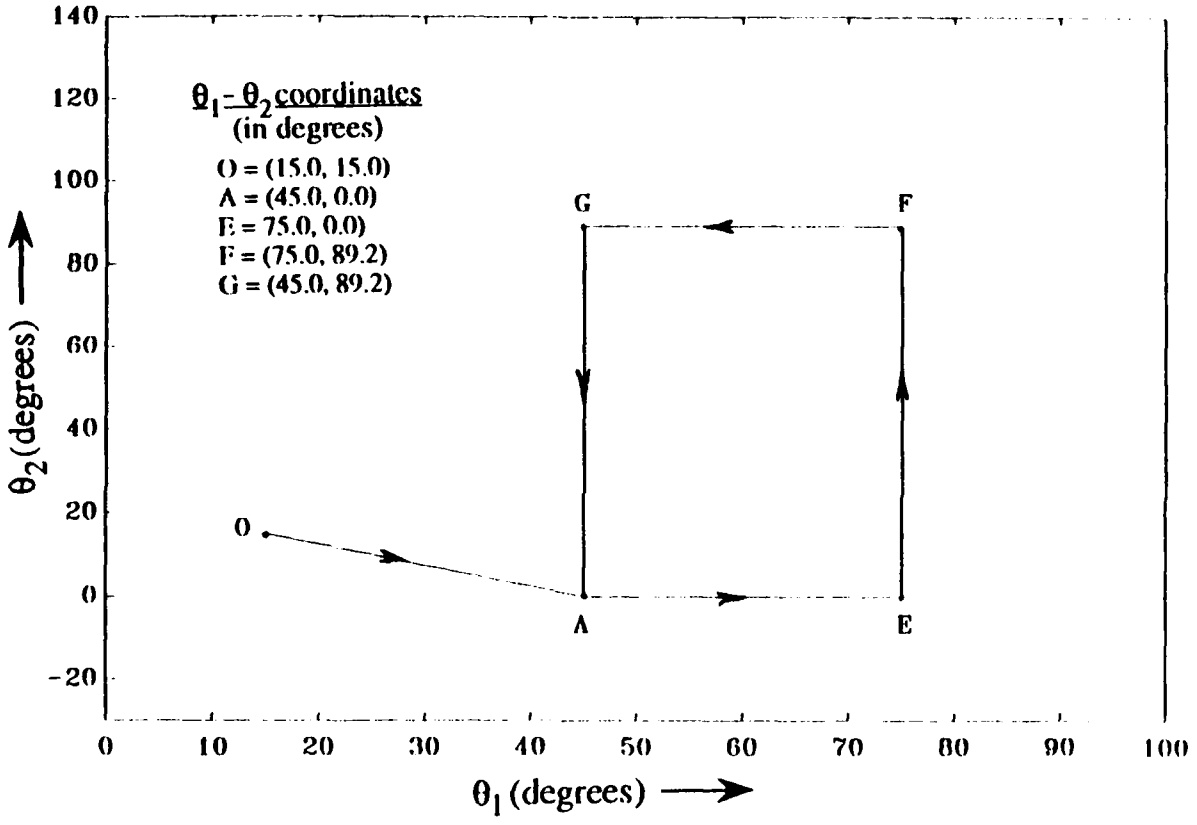

Figure 7(a). The path segment OA followed by the closed trajectory AEFGA converges all of the configuration variables of the space robot to their desired values when the closed trajectory is traversed three times. The closed trajectory was planned subject to the constraint $|\theta_1| \leq 90$ degrees.

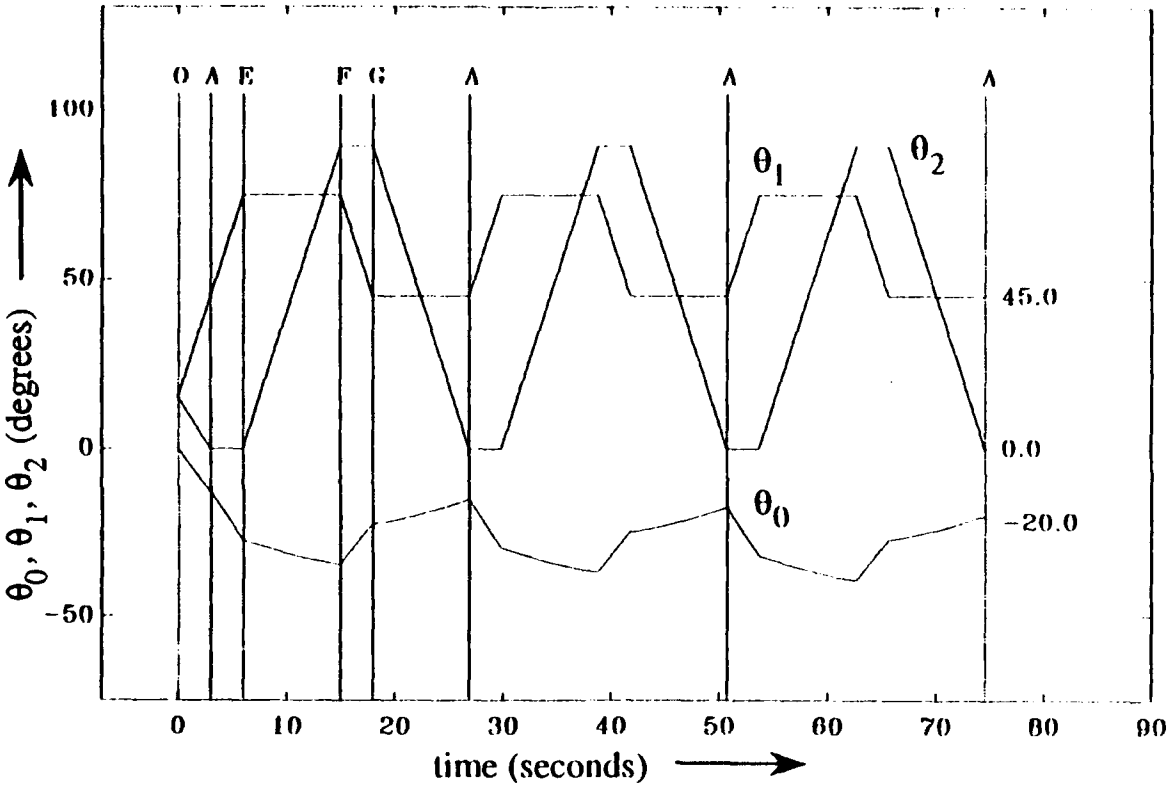

Figure 7(b). Evolution of the configuration variables of the space robot with time when the path segment OA followed by three trips about the closed trajectory AEFGA is executed. The points O, A, E, F, and G in this figure correspond to the same points in figure 7(a).

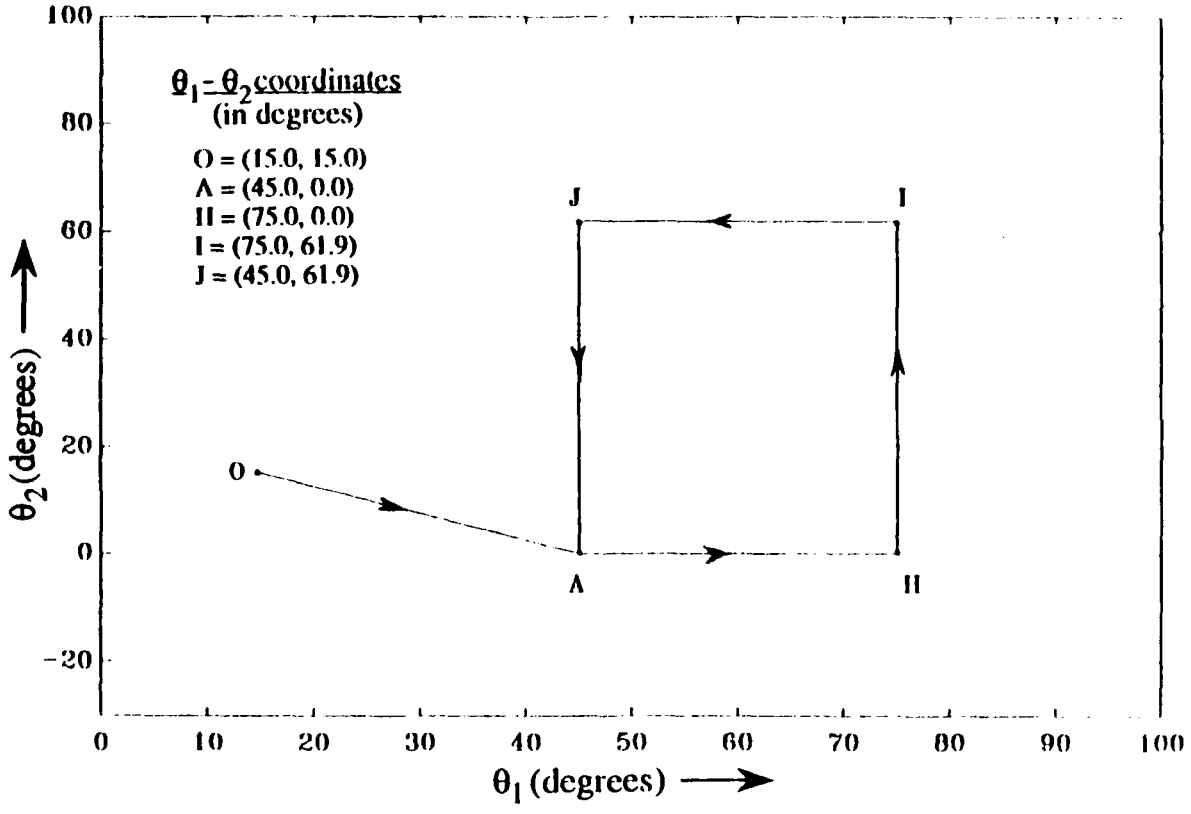

Figure 8(a). The path segment OA followed by the closed trajectory AHIJA converges all of the configuration variables of the space robot to their desired values when the closed trajectory is traversed six times. The closed trajectory was planned subject to the constraints $|\theta_1| \leq 90$ degrees and $|\theta_2| \leq 80$ degrees.

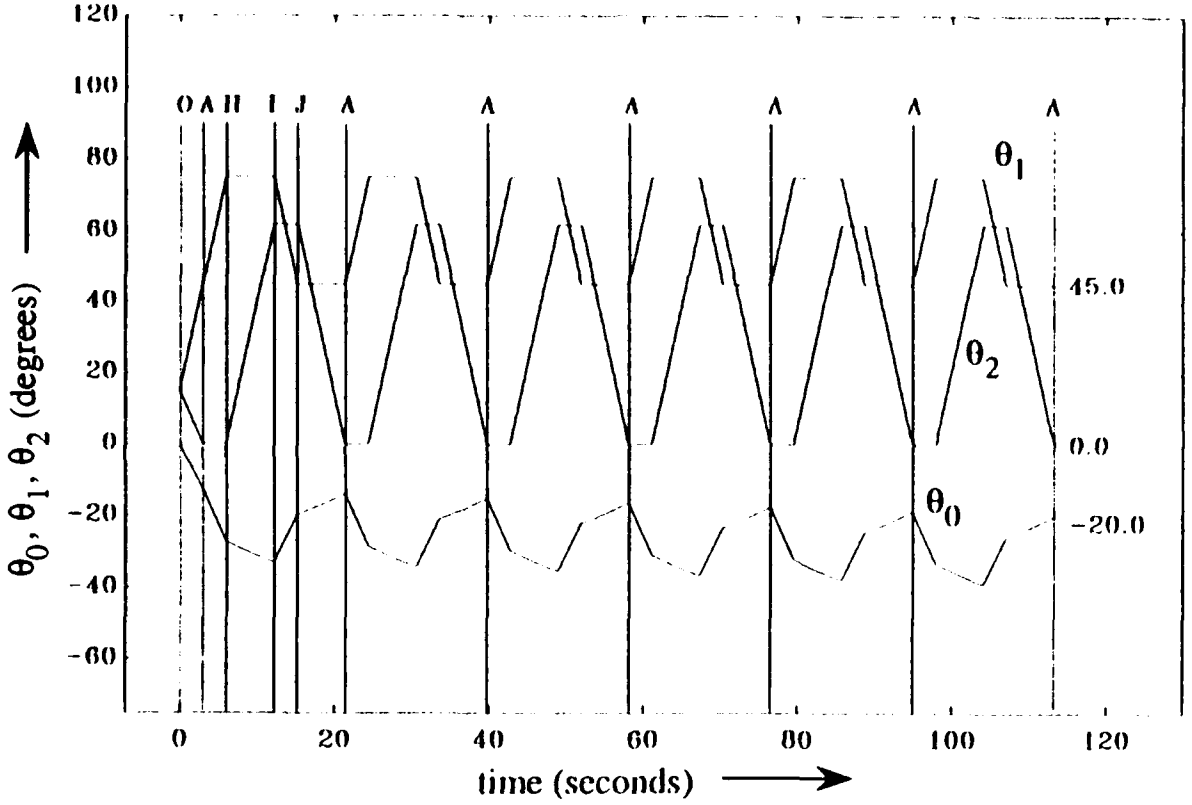

Figure 8(b). Evolution of the configuration variables of the space robot with time when the path segment OA followed by six trips about the closed trajectory AHIJA is executed. The points O, A, H, I, and J correspond to the same points in figure 8(a).

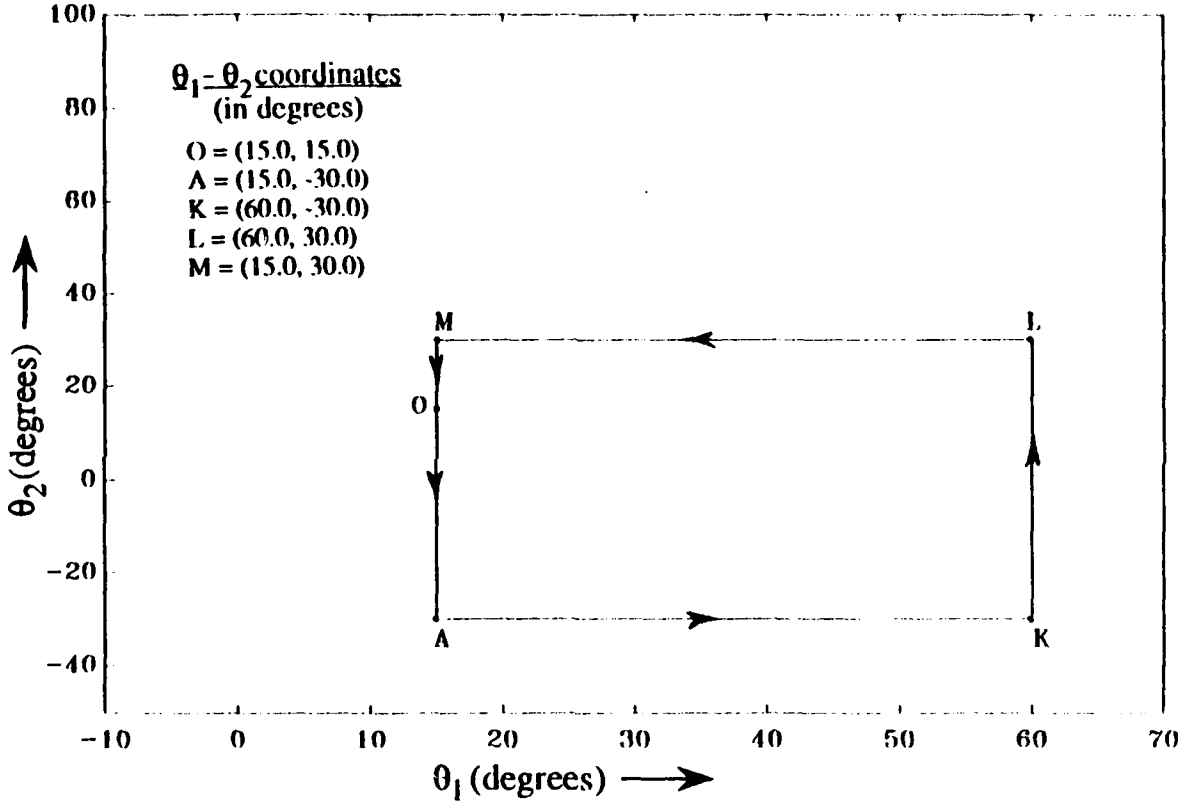

Figure 9(a). The closed trajectory OAKLMO allows the space robot to execute completely repeatable motion between the configuration described by point O and the configuration described by point L.

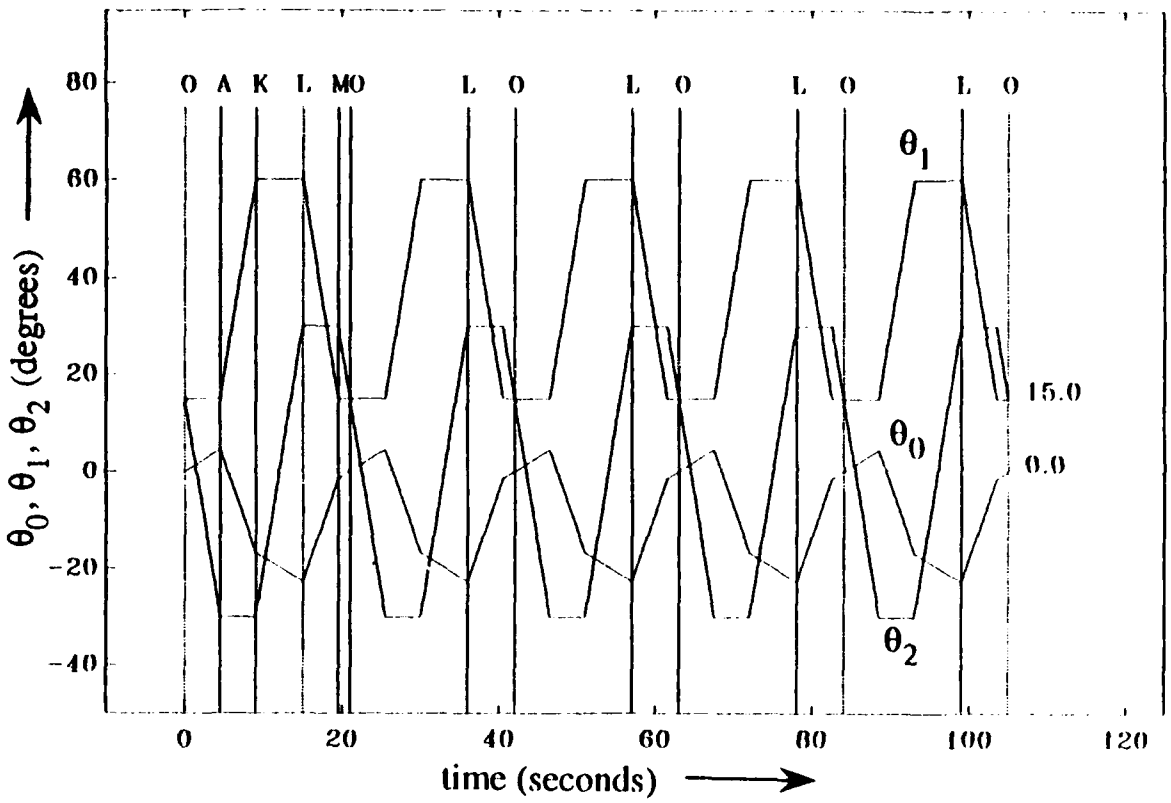

Figure 9(b). Evolution of the configuration variables of the space robot with time when the closed trajectory OAKLMO is executed five times. The points O, A, K, L, and M correspond to the same points in figure 9(a).

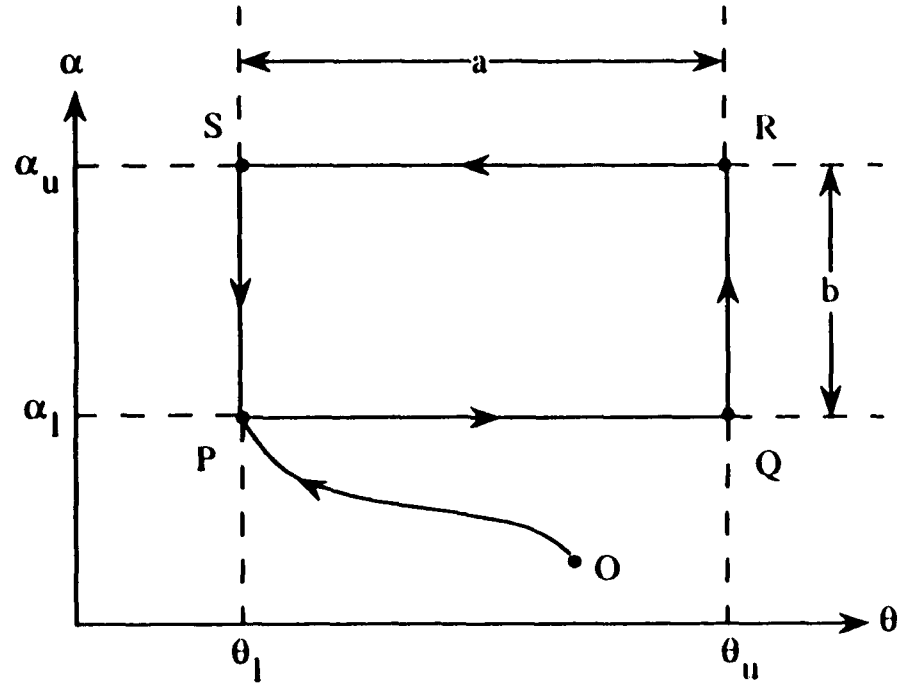

Figure 10(a). An initial path OP and a closed rectangular path PQRSP with sides of length a and b needed to converge the configuration variables of the rolling disk to their desired values. In this figure, α_l has been chosen to be equal to α_f.

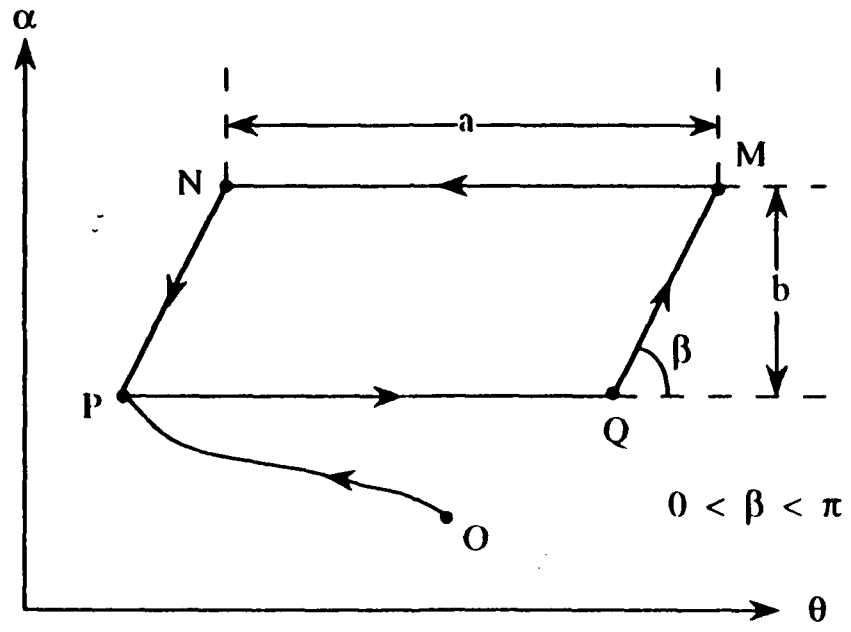

Figure 10(b). The path PQRSP of figure 10(a) can be modified to the path PQMNP shown above. The path PQMNP is a more physically feasible path since it does not require the angle α to change in the absence of rolling.

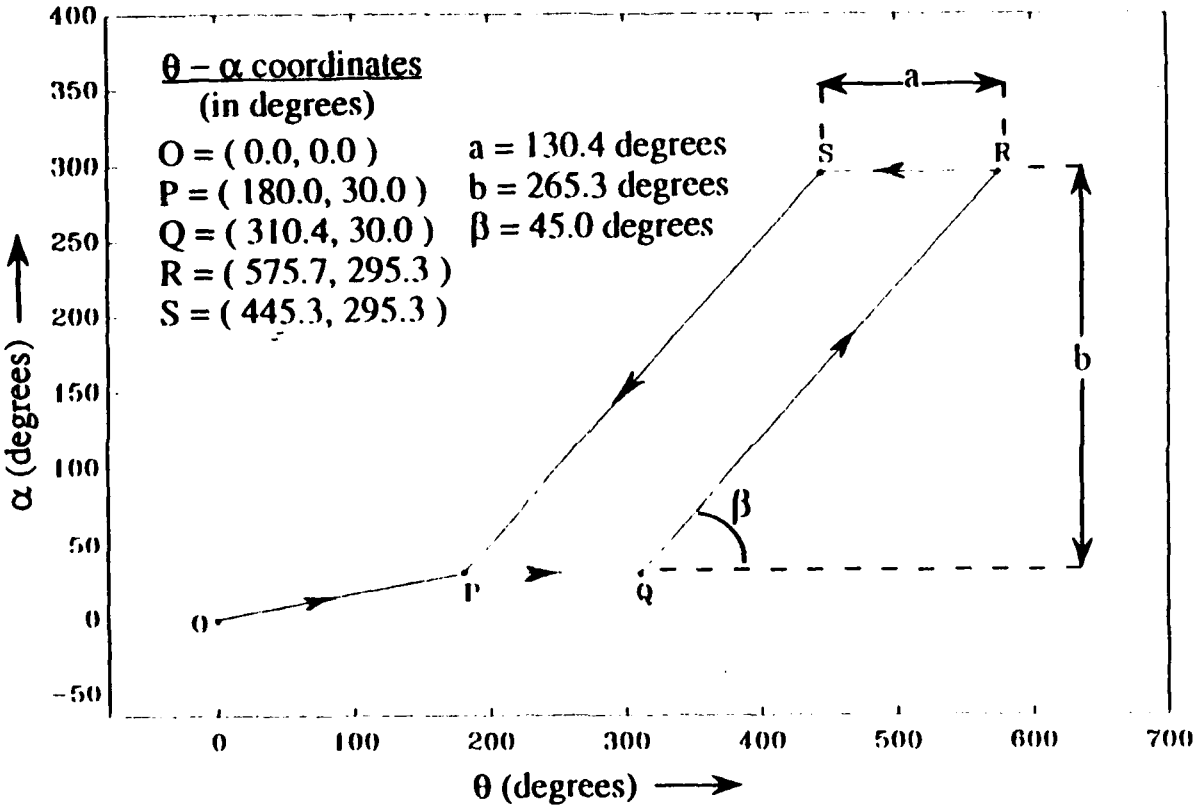

Figure 11(a). The path segment OP followed by the closed trajectory PQRSP converges all of the configuration variables of the rolling disk to their desired values.

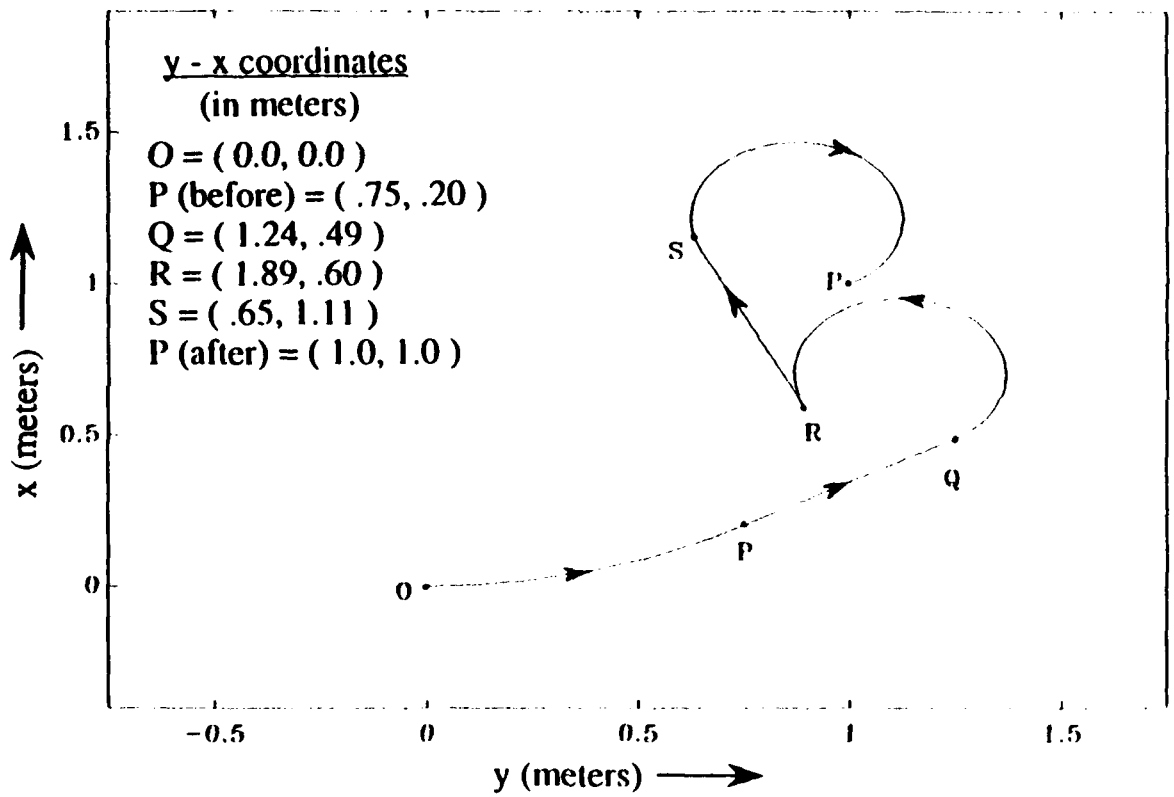

Figure 11(b). The actual path of the disk in the x-y plane. Points O, P, Q, R, S, and P correspond to the same points in figure 11(a).

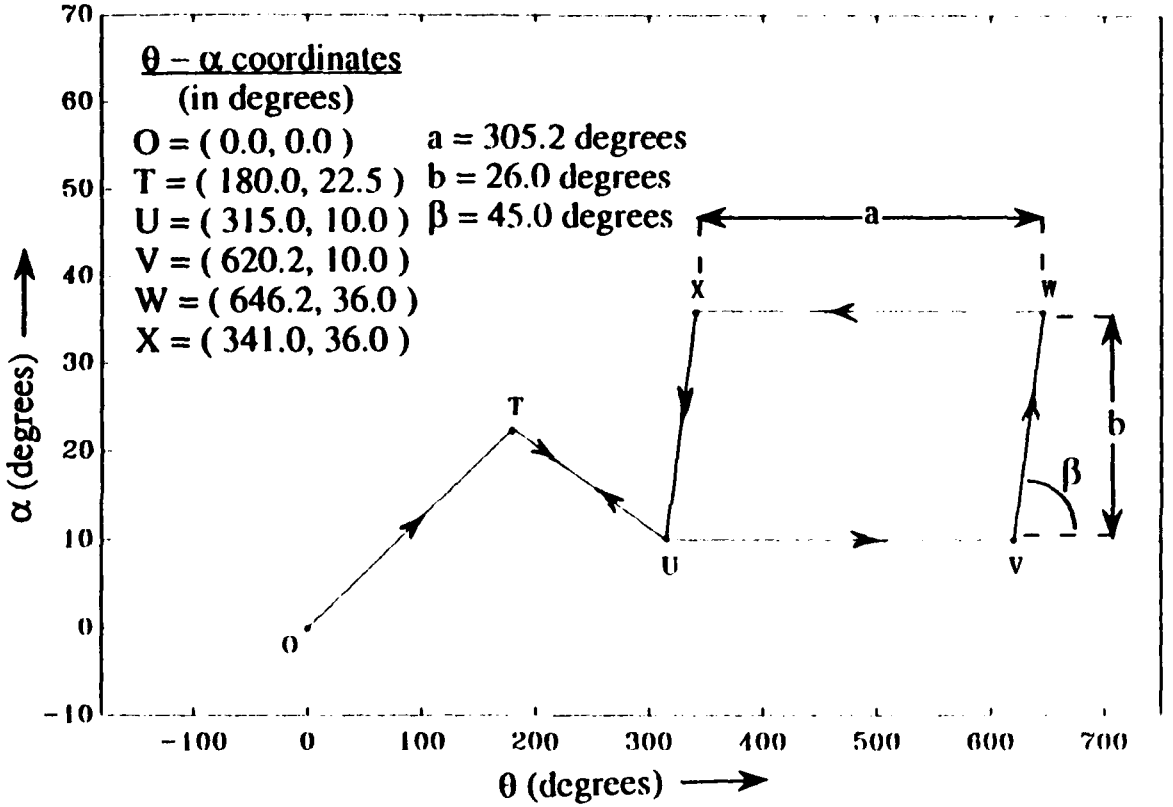

Figure 12(a). The path segments OA and TU followed by the closed trajectory UVWXU and finally back along the path segment UT converges all of the configuration variables of the rolling disk to their desired values. The path segments TU and UT were added to avoid an algorithmic singularity.

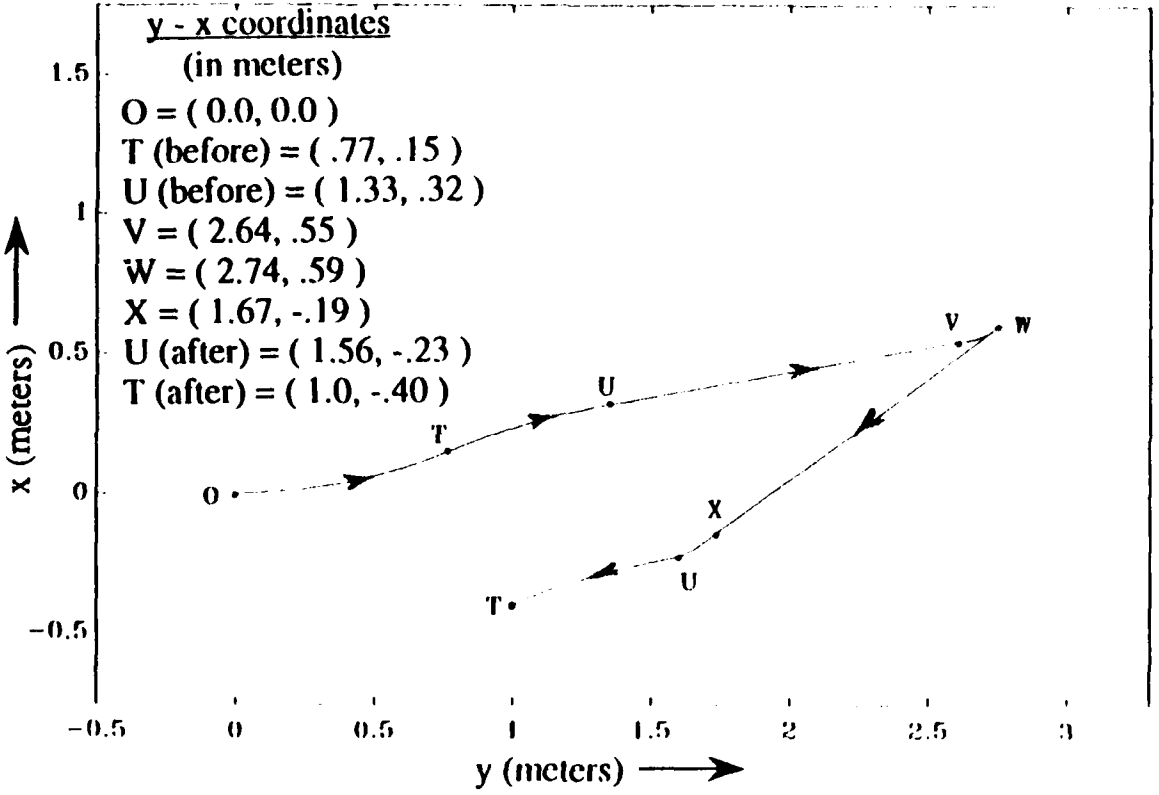

Figure 12(b). The actual path of the disk in the x-y plane. Points O, T, U, V, W, X, U, and T correspond to the same points in figure 12(a).

REFERENCES

1. Kane, T.R., and Scher, M.P., "A Dynamical Explanation of the Falling Cat Phenomenon," *International Journal of Solids Structures*, v.5, pp. 663-670, 1969.

2. Fernandes, C., Gurvits, L., and Li, X.Z., "Foundations of Nonholonomic Motion Planning," paper presented at the IEEE International Conference on Robotics and Automation: Workshop on Nonholonomic Motion Planning, Sacramento, CA, April 1991.

3. Kane, T.R., Headrick, M.R., and Yatteau, J.D., "Experimental Investigation of an Astronaut Maneuvering Scheme," *Journal of Biomechanics*, v.5, pp. 313-320, 1972.

4. Khatib, O., "Real Time Obstacle Avoidance for Manipulators and Mobile Robots," *IEEE International Conference on Robotics and Automation*, pp. 500-505, March 1985.

5. Jacobs, P., and Canny, J., "Robust Motion Planning for Mobile Robots," *IEEE International Conference on Robotics and Automation*, v.1, pp. 2-7, May 1990.

6. Lafferriere, G., and Sussman, H.J., "Motion Planning for Controllable Systems without Drift," paper presented at the IEEE International Conference on Robotics and Automation: Workshop on Nonholonomic Motion Planning, Sacramento CA, April 1991.

7. Murray, R.M., and Sastry, S.S., "Nonholonomic Motion Planning Using Sinusoids," paper presented at the IEEE International Conference on Robotics and Automation: Workshop on Nonholonomic Motion Planning, Sacramento, CA, April 1991

8. Stanford University Technical Report STAN-CS-90-1345, *Nonholonomic Motion Planning versus Controllability via the Multibody Car System Example*, by J.P. Laumond, pp. 1-37, 1990.

9. Cole, A., Hauser, J., and Sastry, S., "Kinematics and Control of a Multifingered Robot Hand with Rolling Contact," *IEEE Transactions on Automatic Control*, v.4, no.4, pp. 398-404, April 1989.

10. Nakamura, Y., and Mukherjee, R., "Nonholonomic Path Planning of Space Robots via a Bidirectional Approach," *IEEE Transactions on Robotics and Automation*, v.7, no.4, pp. 500-514, August 1991.

11. Vafa, Z., and Dubowsky, S., "On the Dynamics of Manipulators in Space Using the Virtual Manipulator Approach," *IEEE International Conference on Robotics and Automation*, v.1, pp. 579-585, 1987.

12. Ince, E.L., *Ordinary Differential Equations*, 1st ed., p.54, Dover Publications, 1944.

13. Kreyszig, E., *Advanced Engineering Mathematics*, 3rd ed., Wiley Eastern Limited, 1972.

INITIAL DISTRIBUTION LIST

1.	Defense Technical Information Center Cameron Station Alexandria, VA 22304-6145	2
2.	Library, Code 52 Naval Postgraduate School Monterey, CA 93943-5002	2
3.	Department Chairman, Code ME Department of Mechanical Engineering Naval Postgraduate School Monterey, CA 93942-5000	2
4.	Professor R. Mukherjee, Code ME/Mk Department of Mechanical Engineering Naval Postgraduate School Monterey, CA 93943-5000	3
5.	Curricular Officer, Code 34 Department of Naval Engineering Naval Postgraduate School Monterey, CA 93942-5000	1
6.	CPT David P. Anderson 389 Kartes Drive Rochester, NY 14616	3